THESIS FOR THE DEGREE OF DOCTOR OF PHILOSOPHY

Chromatographic separation of wood constituents

NIKLAS WESTERBERG

Chemical Engineering
Department of Chemical and Biological Engineering
CHALMERS UNIVERSITY OF TECHNOLOGY

September 2014

Chromatographic separation of wood constituents
NIKLAS WESTERBERG

ISBN: 978-91-7597-051-6

Doktorsavhandlingar vid Chalmers tekniska högskola
Serie Nr 3732
ISSN 0346-718X

Chemical engineering
Department of Chemical and Biological Engineering
Chalmers University of Technology
SE-412 96 Göteborg, Sweden
Telephone +46(0)31-772 1000

Printed by Chalmers Reproservice
Göteborg, Sweden 2014

Chromatographic separation of wood constituents

Niklas Westerberg
Chemical Engineering
Department of Chemical and Biological Engineering
Chalmers University of Technology
SE-412 96 Göteborg, Sweden

Abstract

In a modern kraft pulp mill only about 45 % of the incoming wood is present in the pulp and it is mainly composed of cellulose. The remainder of the wood, which is dissolved in order to liberate the cellulose fibres, e.g., hemicellulose and lignin, ends up in the mill´s recovery boiler to recover the latent energy. The biorefinery concept aims to utilise a larger proportion of the biomass feedstock by converting, for example, hemicelluloses and lignin into new materials, chemicals or fuel.

The research in this thesis investigates the potential and limitations of using chromatographic separation to purify fractions of biopolymers extracted from wood. In contrast to other means of separating wood constituents, chromatography is a highly selective and non-destructive separation process that utilises the species differences in chemical structure. A major drawback associated with this high selectivity is the slow rate of separation, which, in turn, leads to high separation costs. The challenge of using chromatography to separate biopolymers is to develop a method with high specificity while maintaining low costs of separation. To achieve this, a suitable chromatographic system must be developed, static process parameters must be optimised and mass transfer resistance must be minimised.

The findings of this thesis show that wood biopolymers can be separated according to relative contents of aromatic groups using hydrophobic adsorption. It was also found that the solubility of the biopolymers is a limiting factor in the rate of production. Furthermore, calculations indicated that the dominant mass transfer resistance in the system is the intra-particle diffusivity, and therefore the sorbent particle radius should be low (15-20 μm), for an efficient system. Separating larger polymers will also have a negative influence on efficiency, due to dispersive, diffusive, steric and solubility effects. An analysis of the economics involved indicates that the process is not economically viable for the purpose of producing new materials. However, a model system was created that can be used in pre-studies to develop a flexible semi-preparative system for use in fundamental science to better characterise wood constituents.

Keywords: biorefinery, Norway spruce, chromatography, separation, mathematical modelling.

Acknowledgments

This page is dedicated to all of those who helped me finish writing this thesis.

First I want to thank Professor Anders Rasmuson for giving me the opportunity to do my PhD at Chalmers.

All the staff at KAT/KRT and SIKT are acknowledged for technical assistance in the many laboratories I have used.

A special thanks to all my fellow PhD students at Chalmers and within the Wallenberg Wood Science Center, with whom I have shared the trials and tribulations of our work, and to the staff that have encouraged us in times of darkness.

A super-special thanks to my roommate Björn, and my co-workers Olle, Tuve and Hampus. All the tips and our technical discussions are what has brought me this far.

List of Publications

This thesis is based on the following papers, which are attached at the end.

I **Separation of galactoglucomannans, lignin, and lignin-carbohydrate complexes from hot-water-extracted norway spruce by cross-flow filtration and adsorption chromatography**
Niklas Westerberg, Hampus Sunner, Mikaela Helander, Gunnar Henriksson, Martin Lawoko, and Anders Rasmuson
Bioresources 7(4), 4501-4516, 2012

II **Chromatographic separation of wood model constituents - Mathematical modeling and parameter estimation**
Niklas Westerberg and Anders Rasmuson
Chemical Engineering Research and Design 92, 1363-1370, 2014

III **Chromatographic separation of wood model constituents - Analysis and modeling of competing adsorption**
Niklas Westerberg, Björn Lundberg and Anders Rasmuson
Submitted to Chemical Engineering Research and Design

IV **Chromatographic separation of wood constituents - Aspects on process conditions and restrictions**
Niklas Westerberg and Anders Rasmuson
Manuscript

Related work which is not included in the thesis:

i **On the development of a wood based biorefinery**
Wallenberg wood science center, Theme 1.
A demonstrator project where multiple processes were combined to illustrate a modern biorefinery concept.
Manuscript in preparation 2014/2015

Contribution report

The author of the thesis has made the following contributions to the papers:

I Main author. Active in planning the experimental outline, performed parts of the experimental work and the analyses, interpreted the results.

II Main author. Planned the experimental outline, performed the experimental work and the analyses, interpreted the results.

III Main author. Planned the experimental outline, performed the experimental work and the analyses, interpreted the results.

IV Main author. Planned the experimental outline, performed the experimental work and the analyses, interpreted the results.

Paper which is not included in the thesis:

i Planned part of the experimental outline, performed part the experimental work, active in interpreting the results and wrote part of paper.

Contents

Abbreviations

MwD	Molecular weight distribution
LCC	Lignin-carbohydrate-complex
GGM	Galactoglucomannan
WWSC	Wallenberg wood science centre
DP	Degree of polymerisation
LC	Liquid chromatography
HPLC	High performance liquid chromatography
RPC	Reversed phase chromatography
GRM	General rate model
PDE	Partial differential equation
ODE	Ordinary differential equation
ELSD	Evaporative light scattering detector
Da	Dalton
SEC	Size exclusion chromatography
MPM	Mobile phase modifier
HETP	Height equivalent to a theoretical plate
TDS	Total dry solids
MeOH	Methanol
FA	Frontal analysis

Nomenclature

M_W	Da	Molecular weight
d_p	m	Sorbent particle diameter
k_{ads}	$m^{-1}s^{-1}$	Adsorption rate constant
k_{des}	$m^{-1}s^{-1}$	Desorption rate constant
C	mol/m^3	Liquid phase concentration
C_i	mol/m^3	Liquid phase concentration, specie i
q_i	mol/m^3	Solid phase concentration, specie i
q_0	mol/m^3	Maximum solid phase concentration
k_c	m/s	Film mass transfer coefficient
D_e	m^2/s	Liquid diffusivity
D_p	m^2/s	Particle diffusivity
D_{ax}	m^2/s	Axial dispersion coefficient
ε_c	m^3/m^3	Column porosity
ε_p	m^3/m^3	Particle porosity
u_0	m/s	Interstitial velocity
L	m	Column length
P	Pa	Pressure
ΔP	Pa	Pressure drop
$t_{r,i}$	s	Solute retention time
t_0	s	Inert solute retention time
τ	$-$	Tortuosity coefficient
H_i	$-$	Mobile phase modifier coefficient
α	$-$	Relative retention factor
Re	$-$	Reynolds number
Sh	$-$	Sherwood number
Pe	$-$	Peclet number
Pe_p	$-$	Particle Peclet number
Bi	$-$	Biot number

1

Introduction

1.1 General problem area

Concerns have been raised that the rate at which oil can be extracted from the earth´s soil has already peaked, or is likely to do so early in the 21st century (ASPO [1]). To meet the subsequent shortage of resources that will follow this event, there is a general research interest to find ways to replace the petrochemical feedstock with renewable resources. Wood is a renewable resource available in vast quantities, and initiatives are underway to develop new, advanced materials and other products from wood. To meet research needs, the Wallenberg Wood Science Centre (WWSC), a joint research centre run by the Royal Institute of Technology (KTH), in Stockholm, and Chalmers University of Technology, in Gothenburg, was formed with a donation from the Knut and Alice Wallenberg Foundation (WWSC [2]). In 2009, the WWSC launched a material research programme aimed at developing new materials from industrially viable wood species found in Scandinavia.

A number of new material applications of wood polymers have been described and are under development. Examples of uses are hydrogels (Lindblad et al. [3]) and gas barrier films for food packaging, produced both with the hardwood-abundant xylan (Grondahl et al. [4]) and softwood-abundant galactoglucomannans (GGM) (Hartman et al. [5]). Besides the three common components of wood (cellulose, hemicellulose and lignin), studies of the composition of dissolved wood have also found lignin covalently bound to sugars

(Bjorkman [6], Koshijima and Watanabe [7], Azuma et al. [8], Lawoko et al. [9]). Whether these structures exist in native wood, or if this is an artefact of processing is still being debated. The term lignin-carbohydrate complex (LCC) was introduced by Bjorkman [6]. These structures have also presented potential technical applications. Uraki et al. [10] investigated the amphiphilic properties of LCCs and suggested the potential use of LCCs as a polymeric surfactant or as a substance carrier in pharmaceuticals. In addition, Oinonen et al. [11] have reported a method for synthesizing LCC structures and have measured the oxygen barrier properties of polymerized LCC and found them to be similar to the properties of synthesized hemicellulose. LCC is thought to be very diverse in molecular weight and to have aromatic branching on a polysaccharide backbone. If these structures could be separated into pure fractions not only by molecular size, but also by the ratio of aromatic to carbohydrate constituents, more specific material characteristics could be developed.

One prerequisite for material production from wood polymers is the development of methods to separate wood constituents. Commonly employed techniques to achieve such separation are filtration (Persson et al. [12], Andersson et al. [13], Leppänen et al. [14]) and precipitation (Lawoko et al. [9]). The use of filtration is restricted by being chemically nonspecific. Biopolymers from wood can thus only be separated by filtration into fractions of molecules of equal size. Since hemicelluloses and fragments of lignin are often found in the same region of molecular weight, filtration is of limited use when pure fractions of biopolymers are desired. Precipitative separation is based on the solubility of molecules in various solvents. The solubility of a polymer is mainly attributed to its chemical structure, making precipitation a chemically specific method of separation. However; small polymers are less prone to precipitate, and polymers that have a combination of chemical structures have a solubility that differs from pure species. Moreover, precipitation can be irreversible, rendering the precipitated species useless. A third method of separation is sorption. Sorption utilizes the interaction forces between solute species and a solid material that make the species interact (*sorb*) with the surface of the solid phase. Sorption has a much higher chemical specificity than precipitation, but is far more costly. The use of sorptive separation to remove aromatic substituents from industrial waste waters has been summarized by Lin and Juang [15].

It can be concluded that there is a need to develop non-destructive, selective methods to achieve separation of wood constituents. With regard to the purity of the purified fractions; chromatography is probably the method with the greatest potential. The very high specificity of chromatography makes the process suitable for analytical purposes, but it is not extensively employed in biorefinery production due to the high costs associated with the separation process. Therefore, further knowledge is needed about the potential and limitations of the chromatographic separation of wood constituents, and the development of models to be able to analyse the trade-off between productivity and fraction purity, and to scale up the process.

1.2 Objectives

The objective of this thesis is to investigate the potential and the limitations of using chromatographic separation to purify fractions of wood biopolymers.

The scope of the thesis is rather wide, spanning from a proof of concept (Paper I) using extracted wood biopolymers, to an investigation of process parameters by the use of a model system (Papers II, III and IV) and concluding with a viability study in which experimentally verified process conditions were extrapolated to near optimum values (Paper IV).

As a consequence of the broad scope, some factors have been assessed as less important than others and are, therefore, mentioned but not thoroughly investigated.

The thesis aims to answer the following questions: Is separation possible, and what are the crucial parameters that control separation? The thesis also suggests the focus of future research in order to best benefit from the use of chromatographic separation of wood biopolymers.

1.3 Outline of the thesis

Chapter 2 gives an overview of the theoretical background of the thesis, where the basics of wood constituents, and the concepts of chromatography and adsorption are explained, followed by a presentation of relevant transport mechanisms. The mathematical model used in the research is thoroughly explained

in Chapter 3. Chapter 4 explains the methods used in this thesis and the parameter estimation. Some example results of the studies are shown in Chapter 5. Chapters 4 and 5 are presented in the order in which the studies were conducted. The conclusions from the investigations are summarized in Chapter 6, and future research is suggested.

The four papers this thesis is based on, include more detailed information and are attached last.

2

Background

2.1 Wood and wood constituents

The focus of this study is on biorefining constituents from wood. Trees are usually categorised into two kinds: softwood (conifers) and hardwood (deciduous or broad-leaf). In Scandinavia, the trees of the most industrial significance are the conifers; Scots pine (Pinus sylvestris) and Norway spruce (Picea abies). This study is focused on the latter; Norway spruce.

Wood consists of cellulose, hemicelluloses, lignin, wood extractives and some inorganic material. The general composition of these constituents in softwood is 40-46 % cellulose, 23-30 % lignin and 19-26 % hemicelluloses with the remaining few percentages made up of extractives and inorganics (Ek [16]). Investigations into the composition of dissolved wood have also found lignin covalently bound to sugars (Bjorkman [6], Koshijima and Watanabe [7]; Azuma et al. [8]; Lawoko et al. [9]). Whether these structures exist in native wood or if this is an artefact of processing is still being debated. The term lignin-carbohydrate complex (LCC) was introduced by Bjorkman [6]. The findings of Lawoko et al. [9] have even suggested that all hemicelluloses in wood are covalently bound to lignin.

Cellulose, which is the most common compound found in wood, provides structural support in trees. The molecule is a polymer, consisting of 800-10000 repeating units of $\beta - D - glucose$. The number of repeating units is commonly referred to as the *degree of polymerisation* (DP), and this degree decreases during pulping to 300-1700 (Ek [16]). The repeating unit and the low amount

of side groups make the cellulose polymer orient in a crystalline manner, which provides the basis of the strength and support in wood.

Hemicelluloses are also polymers that consist of sugar monomers. The DP of hemicelluloses is much lower than that of cellulose, typically around 100-200. The low DP and the high degree of branching of the polymers make the hemicellulose network structure amorphous. The dominant hemicellulose found in Norway spruce is *galactoglucomannan*, a polymer that consists of monomers of mannose, glucose and galactose, listed here in order of decreasing frequency.

Lignin is a complex polymer oriented in a, seemingly, random network of phenyl propane units. Lignin functions as an adhesive that glues components together into a compound that we call wood.

Lignin-carbohydrate complexes (LCCs) are hemicelluloses that have covalently bonded lignin side groups. The structure, or even existence, of native LCCs is unknown. However, LCCs are usually found in pulping extracts and Lawoko et al. [9] have characterized LCCs as present in the residue of mildly ball-milled wood. LCCs are thought to be widely diverse in DP as well as in the amount of lignin constituents attached to the hemicellulose backbone.

2.1.1 Extractable wood biopolymers

Materials produced from biopolymers exhibit beneficial properties when produced from larger polymers, which means that the value of polysaccharides increases with molecular weight.

Wood polymers, such as galactoglucomannan and LCCs, are extracted from wood by mechanical, thermal and chemical means. The extraction conditions and the wood specie determine the chemical structure of the polymers. Song et al. [17] have extracted Spruce wood and report that the largest average molecular weight distribution (MwD) was obtained by using relatively mild conditions. With higher temperature and longer extraction times, the MwD decreased, while yield increased. The highest MwD of galactoglucomannan obtained was about 35 kDa. Takahashi et al. [18] have reported fractions of LCC polymers with lignin contents ranging between 10-60 % and MwD-averages of 5-500 kDa, from Pine wood. Brownell [19] has managed to characterise LCC polymers with MwD:s between 5-15 kDa, from softwood.

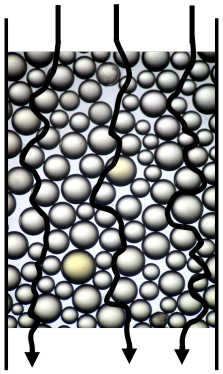

Figure 2.1: Flow through a packed bed

There are pretreatment methods that preserve the native polymer structure in extraction. Azhar et al. [20] have presented a method of enzymatic pretreatment that increases the average molecular weight of polymers in extraction. Jedvert et al. [21] have described a method for exploding wood chips to open up the chip structure, and, thereby, enable extraction at milder conditions.

There are also alternative ways of affecting MwD in the aftertreatment. Oinonen et al. [11] have used enzymes to covalently link LCC polymers together via aromatic groups, and, thereby, increase MwD.

2.2 Chromatography

Chromatographic separation setups always consist of a mobile phase, a fluid, in which the molecules, *solutes*, are transported, and a stationary phase, which the molecules interact with. In liquid chromatography (LC), the stationary phase is usually particulate and contained in a stainless steel column. Figure 2.1 depicts the mobile-phase flow entering the column and flowing in different pathways between the particles.

The particle surface is usually treated to contain molecular groups, *ligands*, of specific characteristics which are to have strong interactions with the molecules that are to be separated. Interaction only occurs when the solutes in the mobile phase come in close contact with the ligands in the stationary phase. Then a weak momentary bonding occurs between solute and ligand (adsorption), before the solute is rereleased into the mobile phase (desorption). The strength of the interaction between solute and ligand varies with the chemistry of the

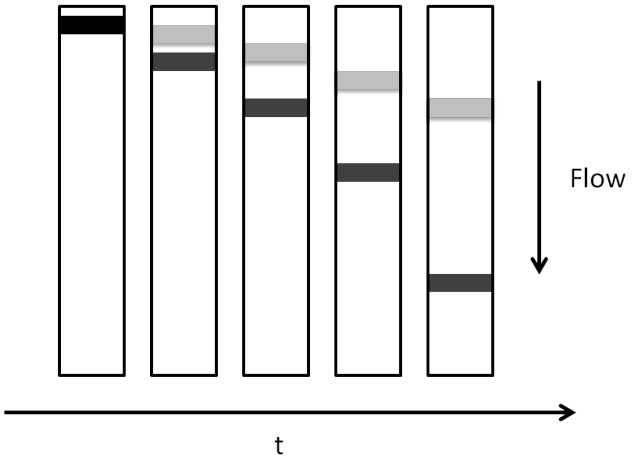

Figure 2.2: Components migrate through the packed bed with different speed, due to different interaction strengths with the stationary phase

solute and the ligand, and also with the chemistry of the mobile phase. Figure 2.2 depicts the migration of two solutes through a chromatographic column.

In this example, the solute indicated by dark grey has weak interaction with the ligands and is, therefore, by preference, located in the mobile phase. The solute indicated by bright grey, however, has strong interactions with the ligands and is, therefore, retained in the column.

This example is a simplified explanation of chromatography. More detailed descriptions of the transport processes that occur in the column and adsorption mechanisms are given below.

2.2.1 Reversed phase chromatography

The separation mechanism in reversed-phase chromatography (RPC) is based on hydrophobic interaction between the hydrophobic solutes in the liquid phase and the immobilized hydrophobic ligands in the stationary phase. Hydrophobic interaction is greater if both the ligands and the solutes are of a phenylic character, due to interaction between π electrons.

2.3 Adsorption

When discussing the fundamentals of adsorption, it is necessary to distinguish between *physical* adsorption and *chemical* adsorption. *Chemisorption* essen-

tially involves the formation of chemical bonds between the sorbate molecule and the surface of the adsorbent. *Physisorption* involves only relatively weak intermolecular forces, making physical adsorption reversible, while chemisorption is often an irreversible reaction.

The distinction between physical and chemical adsorption is conceptually useful, but there are many intermediate cases that might be impossible to categorize exclusively as either one of the two processes. Almost all adsorptive separation processes depend on physical adsorption, rather than chemical sorption. This thesis focuses on physical adsorption.

The interaction forces in chemisorption are strong and involve a chemical reaction between the sorbent surface and the adsorbate. An important example of chemisorption is in heterogeneous catalysis, which involves molecules reacting with each other via the formation of chemisorbed intermediates. The forces involved in physical adsorption include both Van der Waal, dispersion/repulsion forces, and electrostatic interactions comprising polarization, dipole, and quadropole interactions. Ruthven [22] lists the equations that describe these interactions along with a thorough explanation of the process.

2.3.1 Adsorption equilibrium

Adsorption is a dynamic process in which molecules in the solute state continuously transfer to the adsorbed state, and vice versa. In the simplest model of adsorption, in which the adsorption surface is energetically uniform and there is no interaction between the adsorbed molecules, the rate of adsorption, with first-order kinetics, can be expressed as

$$k_{ads}C(1-\Theta) \tag{2.1}$$

$$\Theta = q/q_0 \tag{2.2}$$

where C is the solute concentration in the liquid state, q is the concentration in the adsorbed state and k_{ads} is a constant. q_0 is the adsorption capacity of the sorbent. Correspondingly, the rate of desorption can be expressed as

$$k_{des}\Theta \tag{2.3}$$

With time, the concentration in the two phases will reach equilibrium, when the rate of adsorption equals that of desorption.

$$k_{ads}C(1-\Theta) = k_{des}\Theta \tag{2.4}$$

Expressing the rate constants relation as

$$K = \frac{k_{ads}}{k_{des}} \tag{2.5}$$

gives Equation 2.6 which relates the concentration in the solute state to the concentration in the adsorbed state at equilibrium.

$$\theta = \frac{K \cdot C}{1 + K \cdot C} \tag{2.6}$$

Equation 2.6 is called the Langmuir isotherm. For very low values of C, Equation 2.6 is reduced to the Henry-type, linear equation

$$\theta = K \cdot C \tag{2.7}$$

A number of modifications of the Langmuir isotherm have been proposed to better fit experimental data. The modifications concern additional interaction energies or the surface structure of the sorbent. The experimental data of this thesis was fitted to a number of isotherms, with the best fit to the Tóth isotherm, Equation 2.8.

$$q_i = k_2 \left(\frac{1}{(KC_i)^{k_3}} + 1 \right)^{-\frac{1}{k_3}} \tag{2.8}$$

The Tóth isotherm accounts for adsorption on a heterogeneous surface, with no adsorbate-adsorbate interaction. The heterogeneous surface is assumed to have a unimodal adsorption energy distribution in an interval related to the value of parameter k_3. The Tóth isotherm was first derived for gas-solid equilibria, but like the Langmuir isotherm, it can be extended to liquid-solid equilibrium, (Guiochon et al. [23]).

2.3.2 Competing adsorption

In contrast to the linear conditions of analytical chromatography, large amounts of high concentration feed solution is injected in preparative chromatography, creating non-linear chromatographic conditions, i.e. beyond the linear region of the adsorption isotherm. The concentration of the bands is high during all or most of their migrations, which has several important consequences. First and foremost, the different concentrations move at different velocities. With a favourable isotherm, e.g. the Langmuir isotherm, high concentrations move faster than low concentrations and cause a profound deformation of the elution band profiles. Second, as the isotherms become non-linear, the resin may become saturated and as a result the isotherms become competitive. The components compete for vacant sites in the stationary phase, and as a result, the elution profiles become interdependent, especially for components that elute closely. For these reasons, the equilibrium condition and the mathematical aspects of the theory are much more complex than for linear conditions.

In the event of competing adsorption, the denominator of the isotherm must be a function of all adsorbing species. In a binary system, the Langmuir and Toth isotherms are expressed as Equation 2.9 and Equation 2.10, respectively.

$$q_i = \frac{q_{0,i} k_{1,i} C_i}{(k_{1,i} C_i + k_{1,j} C_j + 1)} \tag{2.9}$$

$$q_i = \frac{q_{0,i} k_{1,i} C_i}{\left((k_{1,i} C_i + k_{1,j} C_j)^{k_{2,i}} + 1\right)^{\frac{1}{k_{2,i}}}} \tag{2.10}$$

2.4 Transport mechanisms

There are a number of transport mechanisms relevant for chromatographic operation. They include: flow, axial dispersion and external/internal mass transfer. Axial dispersion and mass transfer kinetics, in general, cause a broadening of the concentration pulse.

2.4.1 Film mass transfer

The external fluid film resistance around the particles is determined by hydrodynamic conditions. According to the film-theory, a no-slip condition at the solid boundary means that each particle is surrounded by a laminar sub layer. Mass transfer between the bulk fluid and the solid particle is by molecular diffusion through this sub layer. The rate of mass transfer is, thus, determined by the thickness of the sub layer and is more conveniently expressed by an effective mass transfer coefficient, k_c, which is determined by hydrodynamic conditions. According to a linear driving force equation, the coefficient is expressed as

$$V\frac{\partial q}{\partial t} = k_c a_s (C - C^*) \tag{2.11}$$

where a_s is the external surface area, V is the control volume, q is the adsorbed phase concentration averaged over the control volume.

The Sherwood number is a dimensionless group that characterises film mass transfer

$$Sh = \frac{d_p k_c}{D_e} \tag{2.12}$$

where d_p is the particle diameter and D_e is the molecular diffusivity coefficient of the molecule in question in the liquid. As Sh is analogue to the Nusselt number for heat transfer, a lower limiting value of $Sh = 2$ can be found when a particle is surrounded by a stagnant fluid. In a fluid flow, the Sherwood number is expressed as a function of the Reynolds number and the Schmidt number. For low values of the Reynolds number in chromatography, the empirical correlation of Wilson and Geankoplis [24] is useful:

$$Sh = \frac{1.09}{\varepsilon_c}(Re \cdot Sc)^{0.33} \qquad 0.0015 < Re < 55 \tag{2.13}$$

2.4.2 Diffusion

The process in which a concentration gradient is eliminated by random molecular movement, self-propelled by thermal energy, is called *diffusion*. According to Fick's law (Cussler [25]), the diffusion flux is proportional to the negative gradient of concentration. Molecules move from regions of higher concentration

to regions of lower concentration. A distinguishing feature of diffusion is that it results in mixing or mass transport without requiring any bulk motion.

There are two commonly encountered correlations for estimating the diffusivity of dilute species in a liquid. The most common is the Stokes-Einstein equation, especially for large molecules such as proteins or polymers:

$$D = \frac{k_B T}{6\pi\mu R_s} \tag{2.14}$$

k_B is the Boltzmann constant, T is the temperature and R_s is the Stokes radius (hydrodynamic radius) of the diffusing molecule.

$$R_s = \left(\frac{3M_W}{4\pi\rho N_A}\right)^{1/3} \tag{2.15}$$

Wilke and Chang [26] have derived a useful, semi-empirical, expression from large amounts of experimental data, which is often used in contexts of chromatography, Equation 2.16.

$$D_{AB} = 7.4 \times 10^{-8} \frac{(\phi_B M_B)^{1/2} T}{\eta_B V_A^{0.6}} \tag{2.16}$$

where ϕ_B is the association number of the solvent, $M_{W,B}$ is the molecular weight of the solvent, T is the temperature in $^\circ K$, η_B is the solvent viscosity in cP and V_A is the molal volume of the diffusing specie, in cm^3/mol.

Diffusion in porous media

In contexts of diffusion inside porous structures, a distinction is often made between two separate diffusion phenomena: *macropore* diffusion and *micropore* diffusion (Ruthven [22], Suzuki [27], Guiochon et al. [23]). Micropore or intracrystalline diffusion occurs in the volume of the solid, where the diffusing molecule never escapes the force-field of the adsorbent surface. Macropore diffusion takes place in the fluid that fills the pores of the particles. Guiochon et al. [23] have complicated the definition even further by stating that micropores have diameters smaller than 2 nm, macropores have diameters larger than 50 nm, and classifying everything in between as *mesopores*. It might be easier to grasp the difference between macro- and micropores from the hierar-

chical structure of the adsorbents; most commercial adsorbents consist of small microporous crystals that are formed into macroporous pellets or particles.

For macropore diffusion Ruthven [22] distinguishes four separate mechanisms of transport:

1. Molecular diffusion; diffusion in liquid filled pores, where the liquid diffusion coefficient must be corrected with a tortuosity factor to account for three effects that restrict the diffusional flux: i) the random orientation of the pores, which leads to a longer diffusion path than a straight pore would, ii) a reduced concentration gradient in the direction of flow, iii) the variation in pore diameter.

$$D_p = D_e/\tau \tag{2.17}$$

2. Knudsen diffusion; when the pore of diffusion is so narrow that the molecule frequently collides with the wall, thereby reducing velocity.

3. Poiseuille flow; when there is a pressure gradient over the particle that induces an additional acceleration that adds to the diffusional flux. This effect is generally insignificant since the flow resistance in the particles is very large in chromatography.

4. Surface diffusion; refers to when a molecule never leaves the force field of the sorbent surface, but instead jumps between sites available for adsorption. This constricted means of diffusion might make a significant contribution to the flux if the concentration on the surface is very high. The effect is more pronounced if the acting diffusion mechanism is dominated by Knudsen diffusion.

Micropore diffusion occurs by means of the same mechanism as surface diffusion, except in a three-dimensional network in the small micropores, rather than in the larger macropores where this transport takes place on the surface of the pores.

Diffusion of macromolecules

Viel et al. [28] have reported aqueous diffusion coefficients for pullulan stan-

dards of molecular weights between $10^2 - 10^5$ Da, that had been measured with two different methods. According to Viel et al. [28], the diffusion coefficients decrease more rapidly with increasing polymer size than reported by Wilke and Chang [26]. The relation between molecular weight and diffusivity suggested by Viel is presented in Equation 2.18.

$$D_e = 8.2 \times 10^{-9} M_W^{-0.49} \tag{2.18}$$

2.4.3 Axial dispersion

There are two main mechanisms that contribute to axial dispersion: molecular diffusion and the flow velocity distribution in the porous bed. In a first approximation, these effects are additive so that the dispersion coefficient may be represented by Equation 2.19.

$$D_{A,x} = D_M + D_H \tag{2.19}$$

where $D_{A,x}$ is the total dispersion, D_M is diffusivity and D_H is the hydrodynamic contribution.

In liquid systems, molecular diffusivities are too small to make any significant contribution to axial dispersion, even at low Reynolds numbers (Ruthven [22]).

$$D_{A,x} \approx D_H \tag{2.20}$$

If the ratio of bed-to-particle diameter is not sufficiently large the dispersion might increase significantly from wall effects and from non-uniform packing Guiochon et al. [23].

Chung and Wen [29] have reviewed a great amount of published data concerning dispersion in fixed beds and found an expression to estimate the Peclet number as a function of the Reynolds number, Equation 2.21.

$$\frac{Pe\varepsilon_c}{X} = 0.2 + 0.011 Re^{0.48} \tag{2.21}$$

$$Re = \frac{u_0 d_p}{\nu} \tag{2.22}$$

$$Pe = \frac{u_0 d_p}{D_{A,x}} \tag{2.23}$$

where u_0 is the interstitial velocity through the column and X is equal to unity for fixed beds. The correlation by Chung and Wen [29] is applicable over a porosity range of 0.4 to 0.8 with particle density up to 7700 kg/m^3 and Reynolds numbers ranging from 10^{-3} to 10^3. This is the most widely used correlation for estimating dispersion in a chromatographic column when no experimental procedure is available.

The significance of dispersion in a packed bed is described by the Peclet number, defined in Equation 2.23. There is, however, another source of dispersion that can be just as significant. At large particle Peclet numbers, Pe_p, (Equation 2.24), the column advection rate is much higher than the rate of intra-particle diffusion. This causes an inefficient use of the stationary phase since the residence time of the concentration pulse is insufficient to reach equilibration between the phases. A second effect is the added dispersion in the column. The effect of increased dispersion as a function of molecular weight is illustrated in a chromatogram in Figure 2.3. The particle Peclet number can be reduced by using smaller dimension particles, by decreasing the flow velocity or by reducing diffusional resistance. However, a high flow rate is desired to increase productivity, a large sorbent particle diameter reduces the pressure drop in the packed bed and diffusion resistance increases with increasing molecular weight. In other words; there are trade-offs in the optimisation of chromatographic separation.

$$Pe_p = \frac{d_p u_0}{D_e} \tag{2.24}$$

2.4.4 Relative significance of resistances

Large-scale adsorption processes have the practical implication of maintaining a reasonable pressure drop at the relatively high flow rates required. From a process design perspective, this is achieved by using particles with a relatively large diameter in the fixed bed setup. If the interior of the particles has a hierarchical structure, then several diffusive resistances can be distinguished

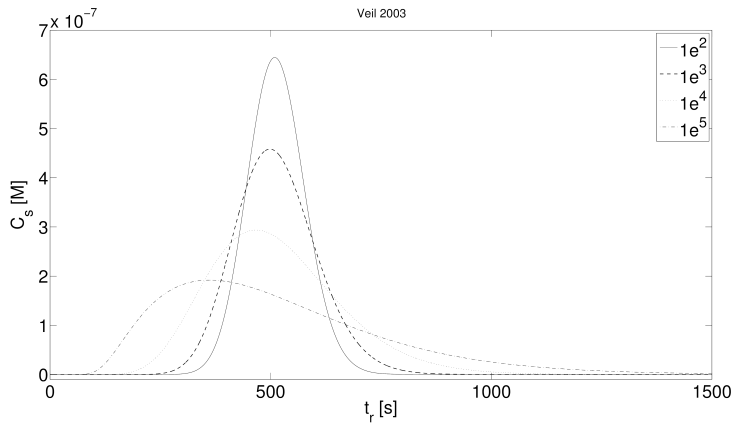

Figure 2.3: Dispersion effect of intra-particle diffusion

in addition to external film resistance. Any single resistance, or more likely, any combination of these different resistances, may control the rate of mass transfer, or at least may have a significant effect on it.

The dimensionless Biot number describes the ratio of internal to external mass transfer resistance, and is defined (for spheres) in Equation 2.25

$$Bi = \frac{k_c d_p}{6\varepsilon_p D_p} \tag{2.25}$$

or in terms of the Sherwood number

$$Bi = \frac{ShDe}{6\varepsilon_p D_p} \tag{2.26}$$

Ruthven [22] argues that since $Sh \geq 2$ and $D_p \leq D_e/\tau$ (where τ is the tortuosity factor, ≥ 1) the minimum value of Bi is $\tau/3\varepsilon_p$ (≈ 3.0). Thus, even at these rather extreme conditions, the internal gradient is clearly larger than the external one. Any additional effects, such as Knudsen diffusion or intra-crystalline diffusion, would add to internal mass transfer resistance. Based on these arguments, it may be concluded that intra-particle resistance is likely to provide the dominant resistance that restricts the rate of mass transfer.

Particle tortuosity, τ, is difficult to measure and could not be distinguished in this work. Tortuosity was, therefore, omitted throughout the work, and effective diffusivity was approximated as equal to the liquid diffusivities of the species.

2.4.5 Flow and pressure drop

Pressure drop in flow through fixed beds has been investigated by a number of authors. Darcy (Darcy [30]) related the pressure drop to the liquid flow through an incompressible bed at low flow rates, Equation 2.27.

$$u = \frac{K}{\mu}\frac{\Delta P}{\Delta z} \tag{2.27}$$

where u is the superficial flow velocity through the bed, μ is the dynamic viscosity of the fluid, ΔP is the pressure drop over the bed when Δz is the length of the bed. K is the permeability of the bed.

In chromatographic contexts, two other frequently referred to investigations related to pressure drop in fixed beds are Chilton and Colburn [31] and Ergun [32]. The data from these and other authors show considerable scatter, although with a common general trend. The scatter is most likely due to wall effects or differences in bed voidage in the different investigations. The data may be conveniently correlated in terms of a dimensionless friction factor, f, defined by Equation 2.28.

$$f = \left(\frac{d_p}{L}\right)\frac{\Delta P}{\rho_f(\varepsilon_c u_0)^2} \tag{2.28}$$

where Δp is the pressure drop (Pa), L is the length of the packed bed, d_p is the diameter of the particulate packing material, ρ_f is the density of the fluid and $\varepsilon_c u_0$ is the superficial fluid velocity.

Chilton-Colburn:

$$f = \begin{cases} 805/Re & \text{Re} < 40 \\ 38/Re^{0.15} & \text{Re} > 40 \end{cases} \tag{2.29}$$

Ergun:

$$f = \left(\frac{1-\varepsilon_c}{\varepsilon_c^3}\right)\left[\frac{150\cdot(1-\varepsilon_c)}{Re} + 1.75\right] \tag{2.30}$$

Both correlations use the Reynolds number based on particle diameter and superficial fluid velocity. Although the expressions are quite different, they show close numerical agreement for a bed voidage of about 0.35. The pressure

drop can be significantly reduced due to wall effects, unless the bed diameter is large relative to particle diameter.

The work in this thesis is solely concerned with laminar flow, i.e., Re $<$ 10.

3

Mathematical model

3.1 The column

The column is modelled as a cylinder filled with particles of equal size. The fluid that flows through the column by means of convection is subjected to small-scale mixing, termed axial dispersion, and is physically depicted using the parameter $D_{A,x}$ (m^2/s).

A shell balance over a thin slice of the column with a constant cross sectional area A (m^2) and a thickness Δ x (m) is used to solve the mass balance for a component in the mobile phase (see fig. 3.1). It is assumed that the packing of the particles is uniform and that the void fraction is independent of the position in the column. Furthermore, adsorption is assumed to occur only inside the particles and is thus solved using a shell balance over the particles (see next subsection). The mass balance for the thin slice is as follows:

$$IN + PRODUCTION = OUT + ACCUMULATION \tag{3.1}$$

Since no reaction occurs in the mobile phase the term PRODUCTION is set to zero. The component is transported in and out of the control volume by means of convection and axial dispersion. Within the control volume, the component is also transported between the mobile phase and the particles of the sorbent. The accumulation term, ACC, is thus a result of the net transport of the component in the control volume.

$$ACC = (IN - OUT)_{Conv} + (IN - OUT)_{Disp} + (IN - OUT)_{Particle} \quad (3.2)$$

The various terms are defined as:

$$ACC = \varepsilon_c \cdot A \cdot \Delta x \cdot \frac{\partial C}{\partial t} \quad (3.3)$$

$$(IN - OUT)_{Conv} = (u_0 \cdot \varepsilon_c \cdot A \cdot C)_x - (u_0 \cdot \varepsilon_c \cdot A \cdot C)_{x+\Delta x} \quad (3.4)$$

$$(IN - OUT)_{Disp} = \left(-D_{A,x}\varepsilon_C A\frac{\partial C}{\partial x}\right)_x - \left(-D_{A,x}\varepsilon_C A\frac{\partial C}{\partial x}\right)_{x+\Delta x} \quad (3.5)$$

$$(IN - OUT)_{Particle} = -(1-\varepsilon_c)A\Delta x\frac{6}{d_p}k_c(C - C_{p,R}) \quad (3.6)$$

where x is the axial coordinate of the column (m), C is the concentration of the solute in the mobile phase (mol/m^3), $6/d_p$ is the specific area of the particles in relation to their volume (m^2/m^3), $C_{p,R}$ is the concentration of the solute at the particle surface (mol/m^3), A is the cross sectional area of the column (m^2), ε_c is the interstitial porosity of the column (m^3/m^3), k_c is the film mass transfer parameter (m/s), Δx is the length of the thin slice (m) and t is the time (s).

Inserting Equations 3.3 - 3.6 in 3.2 gives the following mass balance:

$$\varepsilon_c \cdot A \cdot \Delta x \cdot \frac{\partial C}{\partial t} = \left(-D_{A,x}\varepsilon_C A\frac{\partial C}{\partial x}\right)_x - \left(-D_{A,x}\varepsilon_C A\frac{\partial C}{\partial x}\right)_{x+\Delta x}$$
$$-(u_0 \cdot \varepsilon_c \cdot A \cdot C)_x - (u_0 \cdot \varepsilon_c \cdot A \cdot C)_{x+\Delta x} - (1-\varepsilon_c)A\Delta x\frac{6}{d_p}k_c(C - C_{p,R})$$

Division by $\Delta x\varepsilon_c A$ and letting $\Delta x \to 0$ results in Equation 3.7, commonly referred to as the General Rate Model (GRM) (Guiochon et al. [23]).

$$\frac{\partial C}{\partial t} = -u_0\frac{\partial C}{\partial x} + D_{A,x}\frac{\partial^2 C}{\partial x^2} - \frac{1-\varepsilon_c}{\varepsilon_c}\frac{6}{d_p}k_c\left(C - C_s\right) \quad (3.7)$$

The GRM Equation is subjected to two boundary conditions when solving chromatographic problems. The first boundary condition states that transport to the inlet occurs only through convection, while transport from the inlet

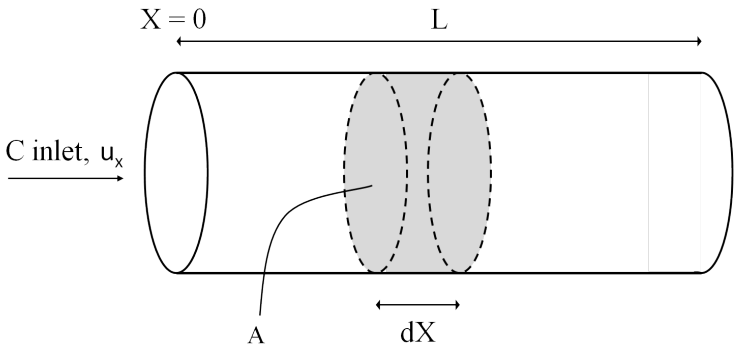

Figure 3.1: A thin slice of the column, over which the mass balance is formulated

occurs through convection and dispersion. This is presented as a mass balance over the volumeless inlet in Eq. 3.8. Accumulation does not occur in this surface.

$$u_0 A \varepsilon_c c_{inlet} = u_0 A \varepsilon_c c - D_{A,x} \varepsilon_c A \frac{\partial C}{\partial x} \text{ at } x = 0 \tag{3.8}$$

Equation 3.8 can be rearranged to give the common Robin condition that describes the column inlet.

$$\frac{\partial C}{\partial x} = \frac{u_0}{D_{A,x}}(c - c_{inlet}) \text{ at } x = 0 \tag{3.9}$$

The second boundary condition is over the column outlet interface, at x=L. Both convective and dispersive transports are taken into consideration at the outlet, whereas only convective transport is considered as leaving the outlet. The concentration is assumed to be the same on both sides of the interface and the following mass balance can be obtained:

$$u_0 A \varepsilon_c c_{inlet} - D_{A,x} \varepsilon_c A \frac{\partial C}{\partial x} = u_0 A \varepsilon_c c \text{ at } x = L \tag{3.10}$$

which can be rearranged into 3.11, a Neumann condition at the outlet of the column.

$$\frac{\partial C}{\partial x} = 0 \text{ at } x = L \tag{3.11}$$

3.2 The particle

The resistance to mass transfer from the surface of the particles to sites of adsorption is described by D_e, the effective diffusion coefficient (m^2/s). Transport within particles can be modeled using a mass balance over a thin radial element of the particle. The particle is assumed to be a sphere of radius R (m) and r is a variable shell radius ($0 < r \leq R$). The thickness of the radial element is Δr (written dr in Figure 3.2). The mass balance is written as:

$$IN = OUT + ACCUMULATION + ADSORPTION \tag{3.12}$$

For simplification, the particle porosity, ϵ_p and the diffusivity are assumed to be independent of the position in the particle. The various terms in Equation 3.12 are:

$$ACC = 4\pi r^2 \varepsilon_p \cdot \Delta r \cdot \frac{\partial C_p}{\partial t} \tag{3.13}$$

$$(IN - OUT)_{Diff} = \left(-D_e \varepsilon_p 4\pi r^2 \frac{\partial C_p}{\partial r}\right)_r - \left(-D_e \varepsilon_p 4\pi r^2 \frac{\partial C_p}{\partial r}\right)_{r+\Delta r} \tag{3.14}$$

$$ADSORPTION = (1 - \varepsilon_p) 4\pi r^2 \Delta r \frac{\partial q}{\partial t} \tag{3.15}$$

C_p is the concentration in the pore liquid (mol/m^3) and $\frac{\partial q}{\partial t}$ is the adsorption rate ($mol/m^3_{solid}s$). Putting together Equations: 3.12-3.15 gives the following expression:

$$\left(-D_e \varepsilon_p 4\pi r^2 \frac{\partial C_p}{\partial r}\right)_r - \left(-D_e \varepsilon_p 4\pi r^2 \frac{\partial C_p}{\partial r}\right)_{r+\Delta r} - (1 - \varepsilon_p) 4\pi r^2 \Delta r \frac{\partial q}{\partial t} = 4\pi r^2 \varepsilon_p \cdot \Delta r \cdot \frac{\partial C_p}{\partial t}$$

Division by $4\pi r^2 \varepsilon_p \Delta r$ and letting $\Delta r \to 0$ gives Equation 3.16 which describes the mass transport within the porous sorbent particles.

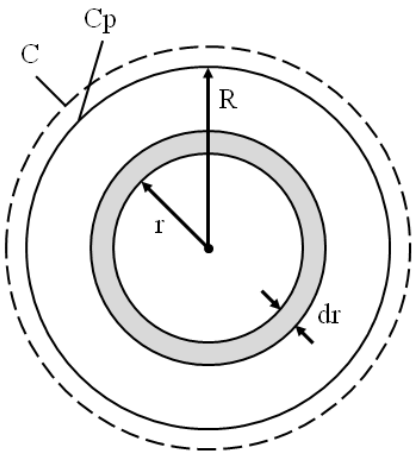

Figure 3.2: Shell balance of a thin slice of a sorbent particle

$$\frac{\partial C_p}{\partial t} = D_e \left(\frac{\partial^2 C_p}{\partial r^2} + \frac{2}{r} \frac{\partial C_p}{\partial r} \right) + \frac{1 - \varepsilon_p}{\varepsilon_p} \frac{\partial q_i}{\partial t} \tag{3.16}$$

This particle model has two boundary conditions. In the first boundary condition, the transport of a component between the particle surface and its surrounding is assumed to take place in a thin film surrounding the particle. Transport from the bulk phase to the particle is then described by Equation 3.17.

$$4\pi R^2 \varepsilon_p \cdot k_c (c - c_{p,R}) \text{ at } r = R \tag{3.17}$$

Transport between the surface of the particle and the interior of the particle is a diffusive process. The diffusive flux from the surface to the interior is described by Equation 3.18.

$$D_e \varepsilon_p 4\pi R^2 \frac{\partial C_p}{\partial r} \text{ at } r = R \tag{3.18}$$

Since there is neither production nor accumulation on the surface, the mass balance of the surface is:

$$4\pi R^2 \cdot k_c (c - c_{p,R}) = D_e \varepsilon_p 4\pi R^2 \frac{\partial C_p}{\partial r} \text{ at } r = R \tag{3.19}$$

Equation 3.19 is equivalent to a Robin condition and is commonly written

$$\frac{\partial C_p}{\partial r} = \frac{k_c}{D_e}(c - c_{p,R}) \text{ at } r = R \tag{3.20}$$

At the particle centre there is no net flux, thus; the concentration gradient equals zero, i.e. a Neumann condition.

$$\frac{\partial C_p}{\partial r} = 0 \text{ at } r = 0 \tag{3.21}$$

3.3 Summary of the mathematical model

Equations describing the transport of a component in a fixed bed flow and the relevant boundary conditions are summarized below.

The equations listed describe the effects of axial dispersion, $D_{A,x}$, film mass transfer resistance, k_c, effective particle diffusion, D_e, and a non-linear adsorption rate equation model.

Equation 3.22 describes the bulk liquid phase in the column with boundary conditions according to Equation 3.23 at the inlet and outlet, respectively.

$$\frac{\partial C}{\partial t} = -u_0\frac{\partial C}{\partial x} + D_{A,x}\frac{\partial^2 C}{\partial x} - \frac{1-\varepsilon_c}{\varepsilon_c}\frac{6}{d_p}k_c\,(C - C_s) \tag{3.22}$$

$$\frac{\partial C}{\partial x} = \begin{cases} \frac{\nu}{D_e}(c - c_{in}) & \text{at x = 0} \\ 0 & \text{at x = L} \end{cases} \tag{3.23}$$

Equation 3.24 describes the fluid-phase concentration in the particles with the boundary condition according to Equation 3.25 at the particle surface and particle centre, respectively.

$$\frac{\partial C_p}{\partial t} = D_e\left(\frac{\partial^2 C_p}{\partial r} + \frac{2}{r}\frac{\partial C_p}{\partial r}\right) - \frac{1-\varepsilon_p}{\varepsilon_p}\frac{\partial q_i}{\partial t}\cdot H_i \tag{3.24}$$

$$\frac{\partial C_p}{\partial r} = \begin{cases} \frac{k_c}{D_e}(c - c_p) & \text{at r = R} \\ 0 & \text{at r = 0} \end{cases} \tag{3.25}$$

The form of Equation 3.24 assumes that the adsorbed species are located in the solid phase. In Equation 3.24, the parameter H_i has been added to describe

the adsorption effect by adjusting the concentration of organic solvent in the mobile phase.

3.4 Multicomponent extension

Adding the effect of competing adsorption to the general rate model requires an increase in numerical effort, since a larger set of partial differential equations must be solved simultaneously.

In Westerberg and Rasmuson [33] (Paper II) the Toth isotherm was found to fit experimental data best, especially at low concentrations where the gradient was found to be very steep. The steepness of this gradient was found to significantly increase the necessary computational time required to find a solution, while the less steep Langmuir isotherm allowed for a more rapid convergence of the calculations.

The diffusive transport in porous particles is described in Equation 3.26. C_p is the pore liquid concentration and r is the radial dimension. This expression includes an equilibrium term involving the slope of the isotherm, $\frac{\partial q}{\partial C_p}$. ε_p is the particle porosity, and is used to correct for the volume fraction pertaining to the solid phase in an expression where the other terms pertain to the pore volume. The parameter H_i is the mobile phase modifier (MPM), which describes the solubility of the solutes as a function of the organic solvent concentration.

$$\frac{\partial C_p}{\partial t} = \frac{D_e}{1 + \frac{1-\varepsilon_p}{\varepsilon_p} H_i \frac{\partial q}{\partial C_p}} \left(\frac{\partial^2 C_p}{\partial r^2} + \frac{2}{r} \frac{\partial C_p}{\partial r} \right) \tag{3.26}$$

Modelling multicomponent isotherms

Two different multi-component isotherms have been tested in this work; the Toth isotherm and the Langmuir isotherm.

The Langmuir isotherm can be extended to account for competitive adsorption in mixtures [34, 35]. The competitive Langmuir model has been extensively used due to its simplicity, but several investigations have reported that the model shows poor agreement with experimental data [23, 36, 37]. Guiochon et al. [23] have listed several extensions of the competitive Langmuir isotherm that show better fit. Cavazzini et al. [38] have compared several competitive

isotherms to describe the separation of enantiomers in a binary racemic mixture, in which the Toth isotherm showed superior fit to experimental data. Cavazzini et al. [38] argue that the superiority of the Toth isotherm is probably due to the model assumption that the resin has a continuous, unimodal adsorption energy distribution, which the Langmuir model does not account for.

In the event of competing adsorption, the denominator in Equation 3.26 must be a function of all adsorbing species. Equation 3.27 shows the expression for a two-component mixture.

$$\frac{\partial q_i}{\partial t} = \frac{\partial q_i}{\partial C_{p,i}} \frac{\partial C_{p,i}}{\partial t} + \frac{\partial q_i}{\partial C_{p,j}} \frac{\partial C_{p,j}}{\partial t} \tag{3.27}$$

The derivatives in Equation 3.27, for the Langmuir isotherm, are derived as

$$\frac{\partial q_i}{\partial C_i} = \frac{q_{max,i} k_i (k_j C_j + 1)}{(k_j C_j + k_i C_i + 1)^2} \tag{3.28}$$

$$\frac{\partial q_i}{\partial C_j} = -\frac{q_{max,i} k_i C_i k_j}{(k_j C_j + k_i C_i + 1)^2} \tag{3.29}$$

The derivatives for the three parameter Toth isotherm are a bit more complex and are presented in Equations 3.30 and 3.31.

$$\frac{\partial q_i}{\partial C_i} = \frac{q_{max,i} k_{1,i} ((k_{1,j} C_j)^{k_{2,j}} + 1)}{((k_{1,j} C_j + k_{1,i} C_i)^{k_{2,i}} + 1)^{\frac{k_{2,i}+1}{k_{2,i}}}} \tag{3.30}$$

$$\frac{\partial q_i}{\partial C_j} = -\frac{q_{max,i} k_{1,i}^2 C_i (k_{1,i} C_i + k_{1,j} C_j)^{k_{2,i}-1}}{((k_{1,i} C_i + k_{1,j} C_j)^{k_{2,i}} + 1)^{\frac{k_{2,i}+1}{k_{2,i}}}} \tag{3.31}$$

3.5 Numerical

The general rate model (GRM), Equations 3.22-3.25, consisting of a set of partial differential equations (PDEs) were solved numerically using the method of lines. The PDEs were discretized to generate a set of Ordinary Differential Equations (ODEs). The set of ODEs was solved using the predefined function ODE15s in Matlab, an implicit, multistep NDF method (Shampine

and Reichelt [39]). A fourth-order-central-finite-difference scheme was used for solving both the column axial domain and the particle domain.

The investigated column volumes in Papers II-IV were discretised with varying accuracy. Discretisation is always subjected to trade-offs between calculus precision and convergence times. Since the computational effort increased from Paper II to Paper IV, the number of discretisation points in the column axial domain and the particle radius were reduced. The reduction in discretised domains had a negative effect on precision, but was found acceptable in relation to convergence times.

4

Methods

4.1 Paper I - Separation of wood constituents

In Paper 1, a simple method for fractionating lignin, hemicelluloses and LCCs from hot-water-extracted Norway spruce was developed. The aim was to separate the constituents according to hydrophobicity, i.e. the amount of aromatic groups relative to carbohydrates.

4.1.1 Experimental method

Sawdust of Norwegian Spruce wood was extracted batch wise in autoclaves. The procedure was adapted according to Song et al. [17] to dissolve material with a preference for the low molecular region; 1-10 kDa.

A cross-flow filtration pilot plant was used for the fractionation of the hot-water extract. The system was operated batch wise and the suspension was circulated across the filter several times. The main advantage of using cross-flow filtration instead of dead-end filtration is that no filter cake is formed. The two-membrane filters used were designed with cut offs at 1 and 5 kDa.

The preparative sorption setup consisted of a glass container containing the suspension, connected via plastic tubing to a high performance liquid chromatography (HPLC) pump. The pump, in turn, was connected via a stainless steel capillary to the column, packed with hydrophobic resin. The outlet of the column was connected to a glass container to collect the permeate or eluate.

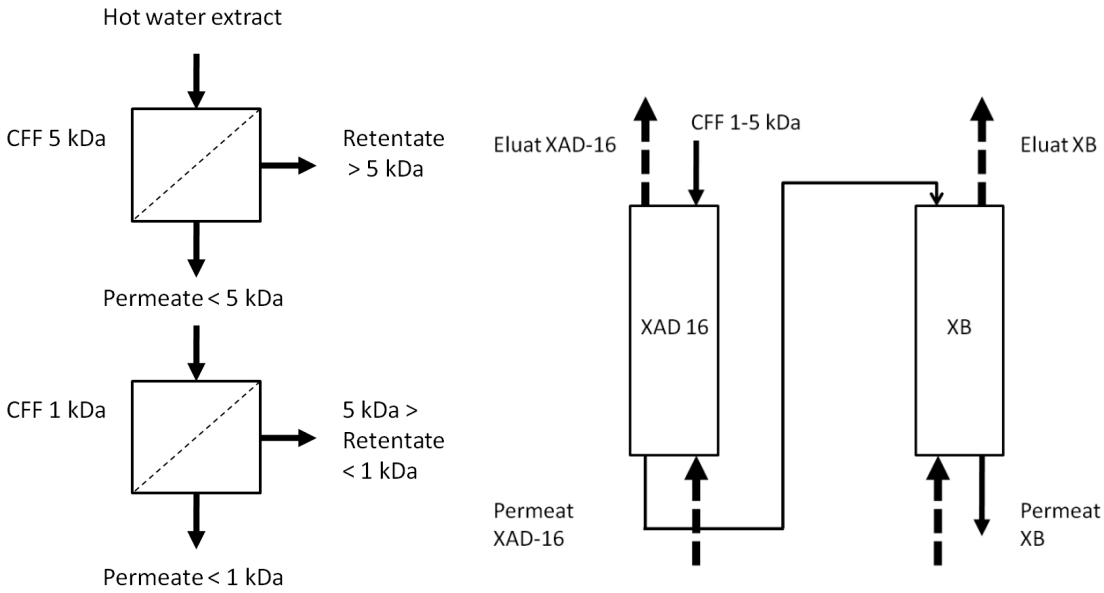

Figure 4.1: Experimental setup in Paper I

The processes of filtration and sorption are illustrated in Figure 4.1. Two different resins were used; a polymeric resin, Amberlite XAD-16, with a styrene divinylbenzene structure, was packed in a 7.8 × 300 mm steel column. The second column was an analytical chromatography column; XBridge Phenyl 5 μm (4.6 × 250 mm). The columns were used in the order depicted in Figure 4.1. The loading and elution steps were performed with low flow rates to ensure that the fluid had time to penetrate the voids in the particles. In the washing sequences, however, the flow rate was increased to the maximum capacity of the pump. The sorptive procedure was executed in a batch-wise sequence to ensure that the capacity of the column was not exceeded. The sequence was: Load - Wash - Elution - Wash.

4.1.2 Characterisation

To characterize the fractions, Klason lignin and sugar content were determined according to the TAPPI test method (1987) T222 OM-83, slightly modified to autoclave at elevated temperature and pressure. For a more comprehensive description of the analytical procedure, see Wigell et al. [40]. The acid-soluble lignin was quantified using spectrophotometry. The molecular weight distri-

bution of the fractions was determined with size exclusion chromatography in a phosphate buffer. Enzymatic hydrolysis of LCCs was carried out with the enzyme NS-51023, Novozymes. The activity of the enzyme had previously been tested according to the method described in Lawoko et al. [41], resulting in verified high hydrolysis on glucomannan and no activity on either lignin, pectin, CMC, or xylan (Y. Wang, pers. comm.).

A more detailed description of the equipment and material can be found in Paper I.

4.2 Paper II - Mathematical modelling and parameter estimation

While Paper I had shown that chromatographic separation of wood biopolymers was possible, the effect of individual physical resistances, or sorptive mechanisms, could not be distinguished. The investigation in Paper II used model compounds to enable the isolation of individual effects.

4.2.1 Experimental setup

All breakthrough and pulse injection experiments were performed in a high performance liquid chromatography (HPLC) setup consisting of a (Waters, Milliford) model 600 gradient pump, an inline degasser, a model 717 autosampler, and an external column temperature controller. For detection, a 2487 dual wavelength detector and a 2424 evaporative light scattering detector (ELSD) were used.

Model compounds and solvents

The model system in this study was meant to resemble the separated species in Paper I to as great an extent as possible. To be able to distinguish the effect of various parameters, the model compounds must be in pure fractions. Obtaining hemicelluloses with a monodispersed degree of polymerization (DP) that carry an exact number of aromatic side groups is difficult, especially if a higher DP is desired. In order to overcome this obstacle, the effect of DP on the retention

mechanism was neglected, and instead, focus was on the aromatic/hydrophobic character of the model compounds.

Salicin is a flavanoid and was chosen as a model compound in this study due to its similarities to LCCs: a sugar monomer with an aromatic side group. Veratryl alcohol (3,4-Dimethoxybenzyl alcohol) was used as a model compound for lignin in this study. Veratryl alcohol is soluble in water and methanol and is more strongly hydrophobic in character than salicin. The chemical structures of these model compounds are illustrated in Figure 4.2.

Blue dextran (Mw 2.000 kDa) is a very large, inert polymer and was used when determining bed porosity and axial dispersion, since steric effects prevent it from penetrating the pores of particles.

In Westerberg et al. [42] (Paper I) acetonitrile was found to be the favourable organic solvent, while the model compounds used in this study displayed higher solubility in methanol. Therefore, throughout this study, methanol was used as the organic modifier, instead of acetonitril.

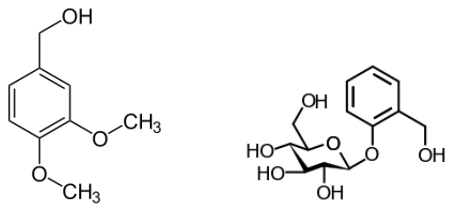

Figure 4.2: Left: veratryl alcohol, right: salicin

Resins and columns

The advantage of using large particle sorbents is a reduction in pressure drop. This reduction allows for a higher production rate in preparative separation. Two batches of granular silica, one with and one without phenyl ligands, were used. The particle size distribution was measured using laser diffraction, and the result is presented in Figure 4.3.

Two porosities were estimated in this study; bed porosity, ε_c, and particle porosity, ε_p. Bed porosity is defined as the void space of the packed column, excluding the void inside the particles. This porosity was estimated by generating breakthrough curves of Blue Dextran, 2MDa. The breakthrough curves

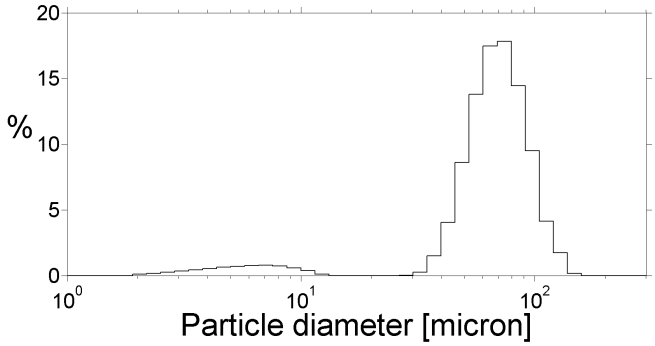

Figure 4.3: Particle diameter distribution

were generated at several flow rates, and an average porosity was estimated from these volumes.

Particle porosity refers to the porous void volume inside the particles and was estimated using the same procedure as above, except using smaller, inert molecules that penetrate and diffuse through the particles.

In addition to these experiments, the solid density of the untreated silica and the phenylic silica was determined using pycnometer measurements. With the solid density the total porosity, ε_{tot} can be determined.

Phenylic silica was loaded in a 4.6×250 mm and a 4.6×75 mm column. The untreated silica was loaded in a 4.6×250 mm column. A vibratory device was used to assist the formation of the bed.

4.2.2 Estimation of parameters

The axial dispersion parameter was estimated by parameter fitting Equation 3.22, without the third term on the right-hand side, to experimental data of pulse injections of Blue Dextran. Pulse injection chromatograms were generated with and without the silica column connected to the system. The pulse injection generated without the column connected to the system was used as input in the simulation. The dispersion parameter in Equation 3.22 was fitted to the generated dispersed pulse. Only the top 80 % of the peaks was used in the fitting, since a tailing effect was observed, which was interpreted as meaning that the tracer interacted with the sorbent particles.

The diffusivity of the species was estimated using the correlation developed by Wilke and Chang [26], Equation 2.16. For comparison, the diffusivity was

also estimated using the Stokes-Einstein equation, Equations 2.14 - 2.15. According to the work of Wilke and Chang [26], as pertains to the solvents used and the molecular weight of the species, the Wilke-Chang equation should be expected to be more accurate than the Stokes-Einstein equation.

The film mass transfer resistance was estimated using the well-known Wilson-Geankoplis correlation (Wilson and Geankoplis [24]), Equation 2.13. The polydispersed particle size distribution makes the use of such a correlation uncertain. The impact of a faulty k_c value was tested with the full model in the verification trials.

A parameter H_i was introduced in Equation 3.24, to account for the effect on the adsorptivity of changes in the concentration of organic modifier in the mobile phase. The effect of organic solvent concentration on the hydrophobic affinity of the analytes was examined using isocratic retention time measurements of pulse injections, with varying concentrations of methanol. The full model (Equations 3.22 - 3.25), including H_i, was fitted to match the retention time of the highest peak. The H_i values were then plotted against methanol concentration and a curve was fitted to that slope.

In addition to affecting the affinity of the solute in the liquid phase, the methanol-water mixture has a different viscosity than pure solvents. The true viscosity of the solvent was estimated by interpolating the data presented in Snyder et al. [43], neglecting the pressure effect on viscosity. The effect of pressure on liquid-state viscosity in methanol-water mixtures has been examined by Kubota and Tsuda [44] who found this effect to be of minor importance. The values of viscosity were measured at 20 °C. The viscosity of the solvent mixture is illustrated in Figure 4.4.

The equilibrium concentration of the solutes in the adsorbed state was measured using breakthrough experiments. The area above the generated breakthrough curve was integrated, and a breakthrough volume was calculated by subtracting the column void and the integrated breakthrough curve generated with no column connected to the system. The total mass adsorbed was calculated with the known liquid-phase concentration. The curve of q_i moles adsorbed to c_i moles/L bulk was then fitted to a number of known adsorption isotherms. After fitting the parameters of the isotherms, the isotherm showing the least residual to the experimental values was used in the model.

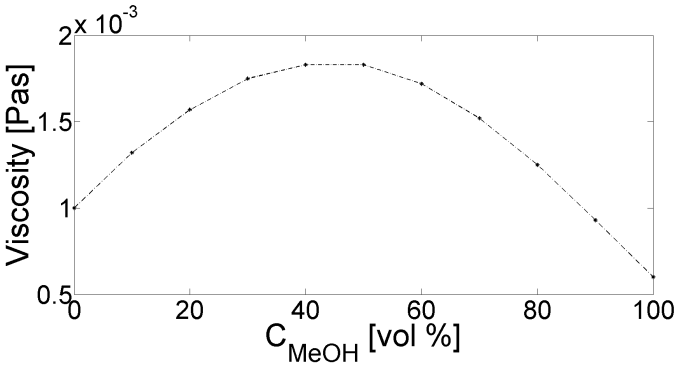

Figure 4.4: Solvent viscosity, effect of MPM-concentration.

4.2.3 Numerical

The estimation of parameters was based on the MatLab function lsqnonlin, a nonlinear least-squares method, which minimizes the residual between the experimental and the simulated breakthrough curve by adjusting the parameters to be estimated in small steps, and moving towards the steepest gradient. The experimental values from injections performed with no column connected to the system formed the inlet concentration to the column in the simulations.

4.3 Paper III - Competing adsorption

The aim of this study was to investigate whether competing adsorption has a significant effect on the preparative chromatographic separation of wood constituents. The effect was estimated experimentally by the use of model compounds. Competitive adsorption was accounted for in a mathematical model of the process using multicomponent Toth or Langmuir isotherms.

4.3.1 Experimental setup and method

Setup

All breakthrough and pulse injection experiments were performed in the same setup as in Paper II.

The same wood model constituents as in Paper II were used in these experiments. The effect of high molecular weight polymers was neglected in this study, because such model compounds could not be found in pure fractions.

Method

In addition to the time- and material-consuming static methods, chromatographic methods are commonly used to estimate competitive adsorption. Both frontal analysis (FA) [45, 46] and pulse techniques [47, 48] can be used to estimate binary competitive isotherms. The most common and validated methods are listed in Guiochon et al. [23], which shows that the FA techniques dominate. The FA techniques are based on an analysis of the shape of successive elution fronts of multiple species, which require the saturation of an entire column. The pulse methods are based on the elution of an adsorbate on a plateau, i.e., a column equilibrated with the other component, at various concentrations.

For this investigation, a dynamic pulse method was selected in which the two components were injected simultaneously at high concentrations. The advantage of this setup is the low amount of solutes that is required, and also that the level of the concentration is low when the peaks reach the detectors, which allows for the use of standard analytical equipment. Under these circumstances, and with this particular experimental setup, the concentrated species will compete for interaction with the stationary phase on the column. As the species progress axially, at different velocities and in reduced concentration caused by dispersion, the competition will decline as the species separate. Thus, competing adsorption only occurs at the beginning of the column, at which point the species occupy the same volume at high concentrations.

The main disadvantage of this method is that the range in which concentration and injection volume can be varied is restricted, and the results are, therefore, not as comprehensive as those obtainable using FA techniques.

Since the effect of competing adsorption is the most pronounced at high solute concentrations and for species with close retention times, HPLC experiments were performed at high concentrations of adsorbates and with low concentrations of organic modifier. One of the reasons that it is so difficult to measure this effect is that, at the high concentrations at which preparative chromatography is run, the effect is the greatest, and the detector response may be beyond its linear region. Thus, when retrieving data from experiments, the registered signal might not correlate with the actual concentrations in the detector.

Experiments were run at three concentrations of organic modifier; 5, 10 and 20 v/v %. Four levels of solute concentrations were tested at these levels. Salicin was varied between 0.0017-0.007 M and veratryl alcohol between 0.008-0.02 M. These are about the highest concentrations that could be used while maintaining solubility and detector response range, while observing competing adsorption effects.

All experiments were conducted using a column with the dimensions 4.6×75 mm prepared with about 0.867 g of irregular phenylic silica resin, as presented in [33]. The flow rate in all experiments was fixed at 1 ml/min.

Calibration considerations

The system dispersion effect was measured by injecting pulses without a column connected to the system. This was performed at low solute concentrations, since only the shape of the elution peak was of interest. For comparison, the shape of an ideal pulse flow was calculated for corresponding flow rates and concentrations, which would produce the same integral as the dispersed peaks. This method showed that the absorption maximum moved towards that of the ideal pulse flow when the injection volume was increased. The procedure is illustrated graphically in Figure 4.5, where the dispersed pulse has been translated into an ideal plug. The results were included as a single-number parameter in the model as a correction factor for off-column dispersion. The values were verified by showing that Equation 4.1 was valid, when Beer-Lambert's law was not, i.e., the integrals of the peaks were proportional to the injected amount, but the peak maximum in the chromatogram was not proportional to the injected concentration.

$$4 \times \int C_i dt = 2 \times \int (2 \times C_i) dt = \int (4 \times C_i) dt \tag{4.1}$$

4.3.2 Parameter estimation

The parameters of the model were estimated in Paper II. However, to improve convergence, the parameters of the isotherms were adjusted in Paper III. The new values are presented in Table 4.1. The new, restricted, regression found in this study led to a minor increase in the residual in the regression. The residual

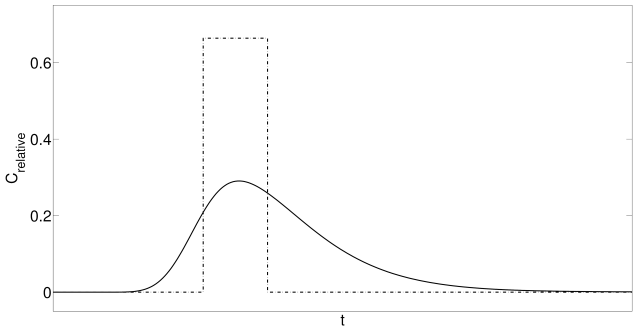

Figure 4.5: Illustration of calculating injection dispersion

increase had an insignificant effect on the model results. The MPM parameters were adjusted accordingly, and the code was adapted to interpolate values instead of fitting regression. The cross-derivative of competing adsorption was set equal to zero for concentrations lower than $C_{min} = 1 \times 10^{-5} M$ for the same reason. To further improve convergence, the Toth isotherms were set as linear below C_{min}.

Solute/model	q_{max}	k_1	k_2
Ver	15.00	28.19	0.2583
Sal	7.996	32.59	0.2432

Table 4.1: Isotherm parameters

4.4 Paper IV - Aspects on process conditions and restrictions

The studies in the previous papers have shown that it is possible to obtain pure fractions of biopolymers by using chromatographic separation based on differences in aromatic content. The physical parameters that describe chromatographic separation were estimated for a model system. The study in Paper IV investigates the influence of sorbent particle diameter and solute molecular weight on separation performance. Productivity estimates were also made, based on verified process conditions and extrapolations of these.

4.4.1 Mass transfer

Dispersion effects in a packed bed are usually characterised by using the Peclet number, Equation 2.23, which compares the rate of advection to the rate of dispersion, where the dispersion term includes axial diffusion in the mobile phase and flow-induced mechanical mixing.

There is, however, another source of dispersion that can be just as significant. At large particle Peclet numbers, Pe_p (Equation 2.24), the column advection rate is much higher than the rate of intra-particle diffusion. This causes inefficient use of the stationary phase since the residence time of the concentration pulse is insufficient to reach equilibration between the phases. A second effect is the added dispersion in the column.

In Westerberg and Rasmuson [33] (Paper II) estimates show that the film mass transfer resistance would be negligible for the system in question.

From Equation 2.13 it is apparent that the coefficient is more strongly dependent on diffusivity than on flow velocity. The separation efficiency impact of film mass transfer was included in the calculations but was not part of the investigation in Paper IV.

4.4.2 Separation efficiency

Elution-data from Westerberg and Rasmuson [49] was used to find an optimal concentration of methanol to achieve rapid separation. The relative retention coefficient, α, was calculated with Equation 4.2. An optimal relation of elution times was found at 11 % MeOH, which was used in all simulations.

$$\alpha(C_{MeOH}) = \frac{t_{r,i} - t_0}{t_{r,j} - t_0} \tag{4.2}$$

Comparison of the height of a theoretical plate (HETP) is a method to evaluate separation efficiency in equilibrium-driven separation processes. With Equation 4.3, the value of HETP can be calculated with experimental or simulated data. A theory of how to minimise the HETP value, and thereby optimise separation, has been described by van Deemter et al. [50].

$$HETP = \frac{L}{8 \times log(2) \times (t_r/W_{1/2})^2} \tag{4.3}$$

where L is the column length, t_r is the retention time of the solute and $W_{1/2}$ is the width of the chromatogram at half height.

For efficient separation, plate height should be low. According to the van Deemter equation, plate height increases with velocity, proportionally to the C term in Equation 4.4.

$$HETP = A + \frac{B}{u_0} + C \times u_0 \tag{4.4}$$

The magnitude of the C term is influenced by the significance of mass transfer resistance at various flow velocities. The term is minimised by minimising the particle radius of the packing material or by decreasing diffusion resistance. In preparative chromatography, it is impractical to operate at a minimum HETP, since this implies a lower velocity and/or low particle radius, and a reduction in the rate of production. The choice of particle radius is restricted by the increase in pressure drop over the column which, in turn, restricts flow velocity. The induced pressure drop, as a function of the flow velocity, column length and particle diameter in a packed bed was calculated with the Ergun equation, Equation 4.5. The purpose of calculating the pressure drop was to ensure that the process conditions were within reasonable limits.

$$\frac{\Delta P}{L} = \frac{150\mu(1-\varepsilon_c)^2 u_0}{\varepsilon_c^3 d_p^2} + \frac{1.75(1-\varepsilon_c)\rho_f u_0^2}{\varepsilon_c^3 d_p} \tag{4.5}$$

4.4.3 Simulations

Simulations were performed using the model presented in Westerberg and Rasmuson [33, 49]. This model was derived with the use of low molecular weight model compounds and was adjusted to consider high molecular weight effects on diffusivity with the empirical relation proposed by Viel et al. [28], Equation 2.18. The model was then used to simulate the chromatographic separation of polymers with molecular weights from 0.1 to 1000 kDa, using sorbent particles with diameters of 5 to 100 μm. The minimum column length to achieve separation was chosen as the response variable, and was calculated from the simulation data. The maximum length of the column simulated was set to 400 mm, to speed up convergence. The procedure was repeated for flow velocities

ranging between 0.00058 and 0.00425 m/s and for purity-restrictions between 90-99 %.

The parameter values at which the simulations were performed are summarised in Table 4.2.

Parameter	Unit	min	max
u_0	mm/s	0.58	4.25
M_W	kDa	0.1	1000
d_p	μm	5	100
Purity	%	90	99

Table 4.2: Simulated parameter intervals

With the estimated process parameters and the assumed biopolymer molecular weights, relative production capacities and corresponding mobile-phase consumptions were calculated for a few different cases that correlated to experimentally verified conditions and extrapolations of these conditions.

5

Results and discussion

5.1 Paper I

The objective of the investigation in Paper I was to test the potential and limitations in a simple laboratory setup to separate hot-water-extracted wood constituents into fractions of hemicelluloses, lignin and lignin-carbohydrate complexes. The main results are presented in Table 5.1.

The complete separation procedure produced three fractions; a retentate on the XAD-16 sorbent, a retentate on the phenylic XB sorbent, and the material that was able to permeate both sorbents without being retained. Throughout the results section, here, these three fractions will be called HWE-XAD, HWE-XB, and HWE-GGM. Hot-water extract, filtered at 1-5 kDa, and the permeate of the XAD sorbent have been included in the analysis as points of reference, and are referred to as HWE-CFF and HWE-XAD-P.

The hot water extraction yielded 144 mg total dry solids (TDS) per gram dry wood (OD) after high-mesh filtration. After cross-flow filtration, the re-

Fraction	Aromatics [wt%]	Yield [mg/g dry wood]
HWE-CFF	5.5	49
HWE-XAD	55.7	1.8
HWE-XB	10.2	1.4
HWE-GGM	1.5	23.7 *

Table 5.1: Summary of main results. * *Estimated from TDS measurements.*

Fraction	Ara	Gal	Glu	Xyl	Man	Klason	ASL
HWE-CFF	3.01	10.42	15.01	11.74	59.82	4.17	1.42
HWE-XAD	1.04	7.32	16.31	2.41	72.92	52.78	2.94
HWE-XAD-P	3.17	10.86	14.72	12.66	58.59	1.02	0.88
HWE-XB	0.20	4.55	18.46	0.55	76.24	8.48	1.71
HWE-GGM	3.42	11.61	14.30	13.99	56.68	0.85	0.69

Table 5.2: Sugar composition in % of total sugars. Klason lignin and acid soluble lignin in wt-% of TDS.

maining TDS amounted to 49 mg g^{-1} where the dead volume of the equipment accounted for a loss of 7.5 mg g^{-1}. The final extract yield was thus 34 %, which confirms that the HWE conditions chosen could dissolve material in this region, as suggested by Song et al. [17]. About 44 % of the TDS was lost in the 1 kDa permeate in the cross-flow filtration.

The composition of sugars, Klason lignin and acid soluble lignin in each fraction are presented in Table 5.2.

The proportion of Man/Glc remained constant at about 4 in all fractions, Table 5.2, which is in agreement with the Norway spruce glucomannan findings of Willfor et al. [51]. Both galactose and arabinose were strongly reduced in content in the retained fractions. About 12 % of the original sugars were xylans. Very small amounts of the xylans were, however, found in the retentates, which led us to believe that the extracted xylan and arabinogalactan were not bound to lignin. However, previous analyses of lignin carbohydrate complexes in spruce have shown that lignin is bound to both xylan and glucomannan (Lawoko [52]). Thus, it is our belief that a major part of the xylan-lignin complex in spruce wood cannot be extracted with hot water at the conditions applied in this study.

The sugar composition remained fairly constant in a comparison of the permeates obtained through adsorptive separation; HWE-CFF to HWE-DAX-P, and HWE-GGM. Data consistently showed that the sugars enriched in the retained fractions were reduced in the permeate fraction, and vice versa. In both retentates, mannose and glucose were enriched, whereas arabinose, xylose and galactose were enriched in the permeates. Following the assumption of Willfor et al. [53] that all mannose is present in galactoglucomannan with a ratio of mannose:glucose:galactose of 4:1:0.5, the sugar part of the HWE-GGM

fraction consisted of about 79 % GGM, and the remainder was xylan and arabinogalactan at a ratio of 2:1.

75.5 % of the Klason lignin and 38 % of the ASL that entered the first sorbent were retained in the HWE-XAD fraction. The XB sorbent reduced the Klason lignin content by 16.6 % and the remainder of the ASL by 21.6 %. The total reduction of Klason lignin was 79.6 %, and the total reduction of ASL was 51.4 %.

The calculated degree of detection, i.e. detectable sugars and lignin, was 80 to 85 % in all fractions. This low degree of detection is likely due to a combination of various measurement errors, mostly attributed to undetected inorganic material in the samples.

Characterization

The HWE-XAD fraction contained mainly lignin, but also a significant amount of sugars. It is our conviction that the fraction consisted of a mix of lignin constituents, LCCs, with a high degree of aromatic side groups, and possibly also hemicelluloses that had been sterically retained in the porous particles and eluted with the adsorbed constituents.

The HWE-GGM fraction was found to consist of mainly sugars. The small amounts of lignin material found in this fraction could be LCCs with a very low degree of aromatic side groups, consequently with high aqueous solubility, and not retained in a hydrophobic resin.

To confirm the existence of covalent bonds between lignin and carbohydrates in the HWE-XB fraction, the method of Lawoko et al. [41] was employed. Size-exclusion chromatography (SEC) was used to estimate the molecular weight (M_W) of the polymers in the HWE-XB fraction before and after enzymatic hydrolysis. The enzyme used was specific in cleaving the mannose-mannose bonds that make up the polymeric backbone of glucomannans. The elution time of the UV_{280} absorbing species was monitored, and it was observed that these species shifted towards a lower M_W after enzymatic hydrolysis, Figure 5.1. Since the enzyme had reduced the molecular weight of the molecules, without any ligninase activity, this meant that the UV_{280} absorbing species must have been bound to the carbohydrates that were degraded.

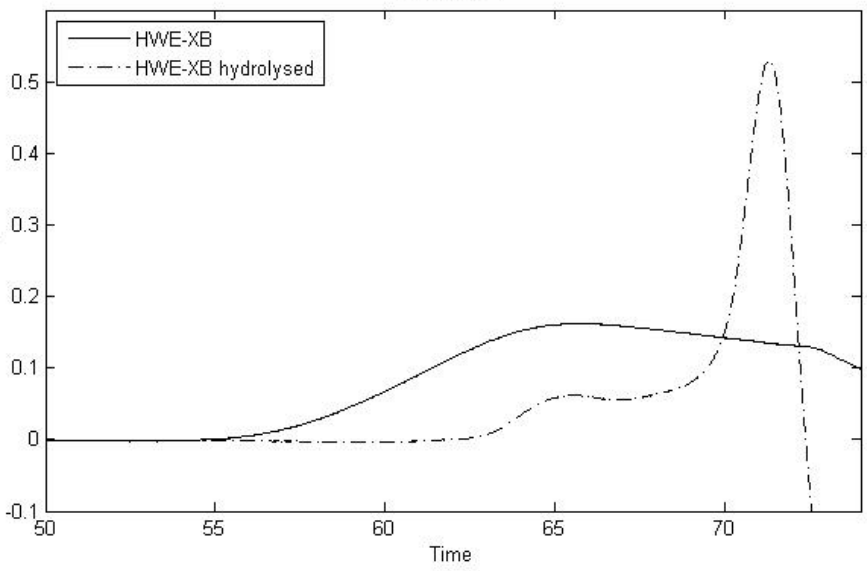

Figure 5.1: HP-SEC curve of HWE-XB fraction. UV detector signal at 280 nm

5.1.1 Discussion - Practical separation

The simple method of fractionating wood constituents using filtration and sorption tested in this study proved successful. Three fractions were obtained and characterized according to each fraction´s main constituent, which was either lignin, hemicellulose or LCC. However, the study also pointed out the limitations of the method. The sorptive sequence of load-wash-elution-wash to maintain the purity of the fractions was very time consuming. Also, the pressure drop over the columns increased significantly during prolonged use. Upon dismantling the columns, the inlet and outlet frits were found to have been severely fouled. Cleansing the frits in heated 0.5 M alkali for 30 minutes removed all visible fouling, and the pressure drop was restored to its original level. Consequently, a proper sequence in preparative separation should also include a cleansing stage. In order to reduce the cycle time, it would be necessary to include an intermediate separation stage prior to the sorptive sequence to remove large lignin structures and inorganic matter, which are suspected of being the fouling species.

Further insight into the sorption behaviour of the species and the transport mechanisms that take place in the column is needed for design and operation purposes.

5.2 Paper II

The objective of the investigation in Paper II was to develop a mathematical model for the chromatographic separation of wood constituents and to estimate the values of transport and adsorption parameters for two model compounds. The resulting parameter values are presented in the text, which is followed by a discussion of the results.

Silica-based sorbents are manufactured as granular particles, a rather crude product unsuitable for analytical chromatography. The reduced specificity of the sorbent is, however, compensated for by a highly reduced manufacturing cost, which could become a significant cost factor in large-scale applications. Another significant aspect is that a larger particle diameter is necessary in large-scale applications, to reduce the pressure drop over the column. Because of this, there is a trade-off between flow rate/production rate and the dispersion mechanisms that reduce separation efficiency.

The values of porosities and particle diameter that were used in the model are summarized in Table 5.3. The values presented in Table 5.3 are the ones used in the modelling. However, salicin exhibited less retention than expected in the phenylic columns. Comparing the Stoke´s radius to the mean pore diameter of the sorbent particles reveals that particle penetration must have been hindered, especially for the slightly larger salicin molecule. To account for the restricted particle penetration found for salicin, an efficiency factor was introduced: $\alpha_{Sal} = 0.83$. This value was obtained by assuming that adsorption/desorption is rapid in comparison to mass transfer, thus neglecting adsorption kinetics totally and fitting particle porosity to the retention time of a low concentration injection of salicin in pure methanol.

Sorbent	Column	ε_C	ε_p	$d_p[\mu m]$
Phenyl	4.6×250	0.35	0.39	68
Phenyl	4.6×75	0.35	0.39	68
Silica	4.6×250	0.35	0.59	68

Table 5.3: Final particle and column parameters used in model

The results from the estimation of axial dispersion are summarized in Figure 5.2, where Equation 5.1 is plotted with the experimental values. Parameter

fitting of pulse injection curves resulted in a linear curve for the narrow Re interval investigated. The curve was in the same range as predicted by Chung and Wen [29], Equation 2.21, but increased more rapidly with increasing Reynolds number.

$$D_{A,x} = 2.97 \cdot 10^{-6} \cdot Re + 0.127 \cdot 10^{-6} \qquad m^2/s \tag{5.1}$$

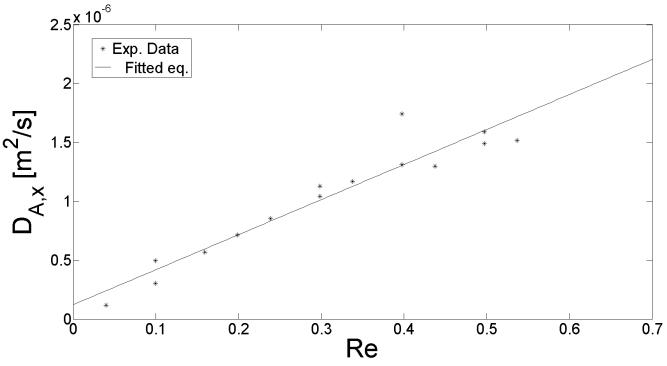

Figure 5.2: Axial dispersion coefficient as a function of Reynolds number

The results from calculating the diffusivities using the method of Wilke and Chang [26] are presented in Table 5.4. According to Wilke and Chang [26], as pertains to solvent and solute properties, the Stokes-Einstein correlation underestimates diffusivity, resulting in values of about one order of magnitude lower.

Solvent	Veratryl	Salicin
Water	7.5	6.1
Methanol	8.5	7.0

Table 5.4: Diffusivities in $\times 10^{-10}$ m^2/s

The H_i values fitted to retention time measurements are plotted in Figure 5.3, along with the fitted Equation 5.2. Equation 5.2 was adapted from Melander et al. [54], and includes both hydrophobic and electrostatic interaction. While this physical interpretation might be somewhat inaccurate for this system, the expression fits the experimental values well.

$$log(H_i) = \alpha_1 + \alpha_2 log(C_{MeOH}) + \alpha_3 C_{MeOH} \tag{5.2}$$

The adsorption equilibrium data was fitted to several known isotherms. A three-parameter isotherm proved necessary to fit the data, and the Tóth isotherm showed the best fit, Equation 2.8. The fitted isotherms of the species are plotted with the experimental data in Figure 5.4. The Tóth isotherm is reduced to a Henry-type equation at low concentrations, and this was used in simulations to avoid numerical difficulties.

Verification of the model

The model developed was verified experimentally on the 75×4.6 mm phenylic silica column. The experimental pulse injections were compared to the corresponding curve simulated with the model. The model was verified by estimating the error in the predicted elution volume. In addition, the shapes of the injection pulse and the corresponding simulated curve were compared and the possible sources of inconsistency were listed.

The elution volume error average was calculated with Equation 5.3.

$$\overline{R} = \frac{\sum |1 - t_{r,sim}/t_{r,exp}|}{n} \tag{5.3}$$

where t_r is the retention time of the highest peak for the simulated and the experimental pulse, respectively, and n is the number of experiments. The model was found to be accurate to within 95 % in regard to the elution volume.

When the parameters were estimated individually, the simulated peak shape was close to perfectly Gaussian. The experimentally generated peaks, however, exhibited a *fronting* behaviour, where a part of each peak eluted at a lower

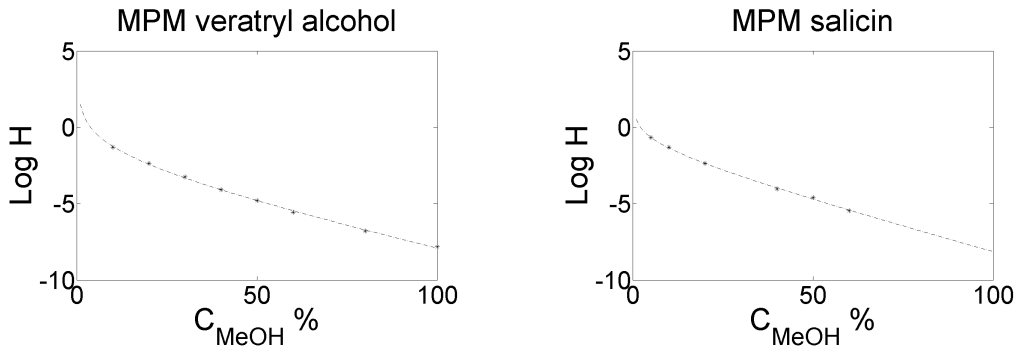

Figure 5.3: Effect of mobile phase modifier. Left: veratryl alcohol, right: salicin

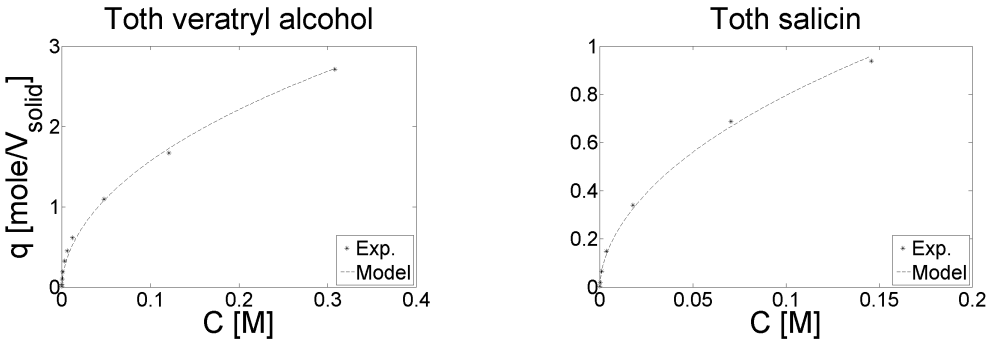

Figure 5.4: Tóth isotherms of veratryl alcohol and salicin

volume than the one calculated. This observed phenomenon was interpreted as *channelling*. An alternative explanation for this phenomenon is that some of the particle pores had been plugged, or $fouled$, which would have a similar effect on peak shape.

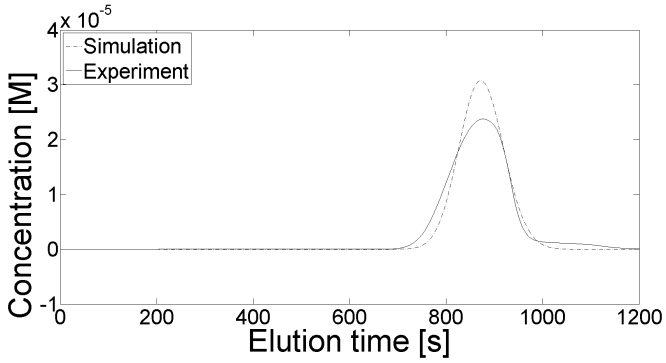

Figure 5.5: Example of simulation versus experimental elution

5.2.1 Discussion - Modelling

The objective of the study in this paper was to create a mathematical model of chromatographic separation of wood constituents for a simplified model system. The purpose of the model was to evaluate how various parameters influence this separation and, with this knowledge, to find the optimal operational conditions for preparative separation.

The Biot number was used to compare external with internal mass transfer resistance (Equation 2.25). k_c varied with flow rate, while the particle diameter was fixed in the investigation and D_e varied only slightly with the solvent used.

The Biot number was in the range of 10-20 in this study, which means that the internal mass transfer resistance was dominant.

The kinetics of adsorption/desorption was neglected here. This simplification was suggested by Ruthven [22] who argues that physical adsorption-/desorption rates are much faster than internal and external mass transfer rates. The hydrophobic affinity to the stationary phase was stronger for veratryl alcohol than for salicin, as predicted by Westerberg et al. [42] and Takahashi et al. [18]. The solubility in mixtures of water and methanol is well described by the mobile-phase-modifier parameter; H_i. The estimated adsorption isotherms match the experimental values well, and the column and particle porosities, ε_c and ε_p, were determined using two methods. The weakest part of the model seems to be the mechanical dispersion effect. The verification tests showed that the elution curves were fronting. A comparison of the elution volume to the column volume confirmed that this was not a kinetic effect. The effect is called "*channelling*", but whether the origin of this is in the bed structure or in particle pores is unclear.

The system of chromatographic separation of wood constituents was, in this study, highly simplified in order to be able to evaluate the individual parameters of separation. Only one type of sorbent material, one kind of organic solvent, and only two model compounds were selected to resemble the constituents of wood. The largest deviation of the model from a real case separation procedure was in the chemical structure of the constituents. The lignin-carbohydrate bonding scheme is not well understood, and the structure of the water-soluble lignin fragments, produced when dissolving wood, are complex and diverse. The number of aromatic side groups of the LCCs controls the adsorption on a hydrophobic resin, as shown by Takahashi et al. [18] and Westerberg et al. [42], while the molecular weight of the molecules has a major influence on which sorbent geometry to use and then, especially, the diffusivity of the species. The value of the biopolymers increases by molecular weight (M_w) and purity (monodisperse aromaticity), which places high demands on processing costs.

Preparative chromatographic separation is, in practice, operated at high concentrations, while this study was conducted at low concentrations. The effects of high-concentration separation should be studied prior to designing a preparative separation unit.

5.3 Paper III

The aim of Paper III was to investigate the effect of competing adsorption in chromatographic separation of wood biopolymers, and to investigate how this phenomenon can be modelled.

The effect of competing adsorption is visible in a chromatogram as a reduction in retention times, especially concerning the less retained species when there is a large difference in affinity for the stationary phase. An example is shown in Figure 5.6. The experiments showed that the effect of competing adsorption was more pronounced in samples with higher concentrations of solutes and eluted with lower concentrations of the organic modifier. At 20 v/v % MeOH there was virtually no sign of competing adsorption, as there was with the lowest concentration of solutes.

The method chosen to present the results compares the efficient adsorption volume for the less retained species, by evaluating the reduction in efficient column volume as a function of sample injection volume and sample concentration.

The value was calculated as a percentual decrease in efficient column volume (ΔV) and was calculated with Equation 5.4.

$$\Delta V = \frac{V_{single} - V_{CA}}{V_{single}} \tag{5.4}$$

where V_{single} is the volume of the mobile phase required to elute the single-component injection, and V_{CA} is the volume of the mobile phase required to elute the same component influenced by competing adsorption. Mobile-phase volumes were calculated with Equation 5.5.

$$V_i = F \times t_{C_{max,i}} \tag{5.5}$$

where F is the flow rate, $t_{C_{max}}$ is the point in time at which the chromatogram shows maximum absorbance. The concept of the (ΔV) calculation is illustrated in Figure 5.6.

Several methods for analysing and presenting the findings were tested in which the entire elution curve was used. One problem was that the experiments

that included competing adsorption showed a tailing characteristic, which prevented any comparison to the reference curve.

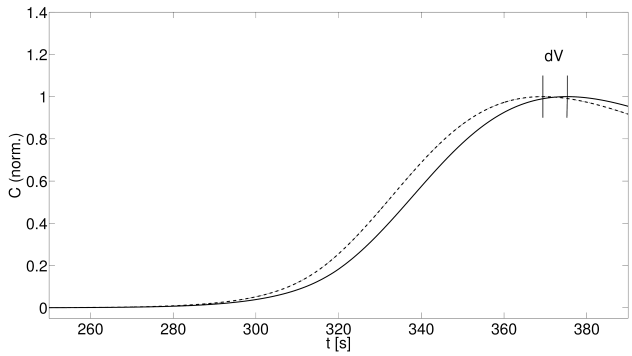

Figure 5.6: Example of calculating loss of efficient column volume

5.3.1 Experimental results

The experimental results are presented in Figure 5.7 as a percentual reduction of the effective column volume as a function of injection volume and of sample concentration, for 5 and 10 % methanol as the mobile phase. Higher resolution images are found in Paper III.

The results from using 20 % organic modifier have been omitted, since no effect of competing adsorption could be observed.

Figure 5.7 clearly shows that the effect of competing adsorption increases with injection volume and injection concentration. Percentually, the effect is only slightly higher for lower concentrations of organic modifier.

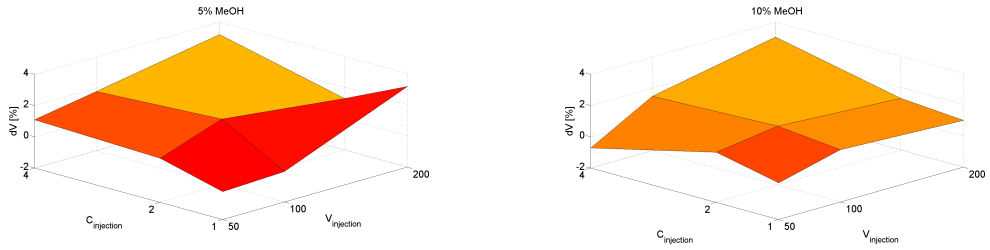

Figure 5.7: Experimental results - column reduction

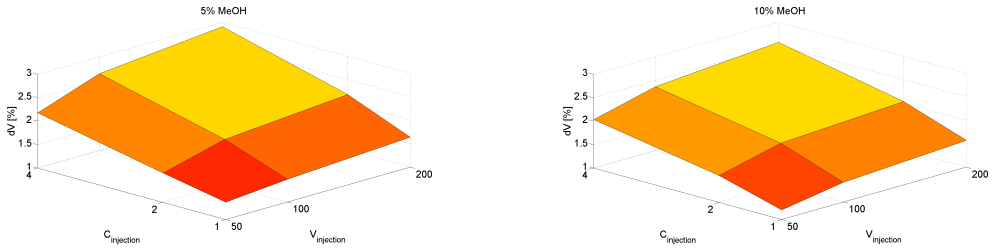

Figure 5.8: Simulation results - column reduction, Toth isotherm

5.3.2 Simulation results

Simulations were performed within the same concentration region as the experiments. The results were recalculated using Equation 5.4, and are presented in Figure 5.8 to be comparable to the results of the experiments.

Simulations using the modified Toth isotherm show very good agreement with the experimental results. The Langmuir isotherm underestimated the effect to such an extent that it could not be used to model the phenomenon, and is therefore not included in the figures. The explanation for the differences in ability to predict competing adsorption are due to the shapes of the isotherms. The Langmuir isotherms were plotted with respect to both components in Figure 5.9, and the Toth isotherms were plotted in Figure 5.10. Higher resolution figures are found in Paper III. While the effect of competing adsorption increases rapidly with concentration and reaches a plateau value in the Toth isotherm, as can be seen, the effect was clearly weaker in the Langmuir isotherm, and appears linear in the region examined.

The resolution of the competing adsorption effect came at a cost of 3-4 times longer computational time, due to the complexity of the Toth isotherm and the steepness of the isotherm at low concentrations.

In conclusion, the results from experiments and from simulations with the Toth isotherm coincide well, both in order of magnitude and in general trends. The general trends are:

- Higher concentration of solutes leads to a larger reduction in the effective column volume.
- Greater injection volume leads to a larger reduction in the effective column volume.

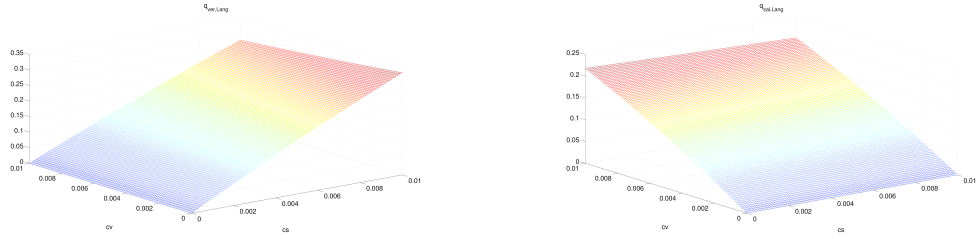

Figure 5.9: Langmuir binary isotherms

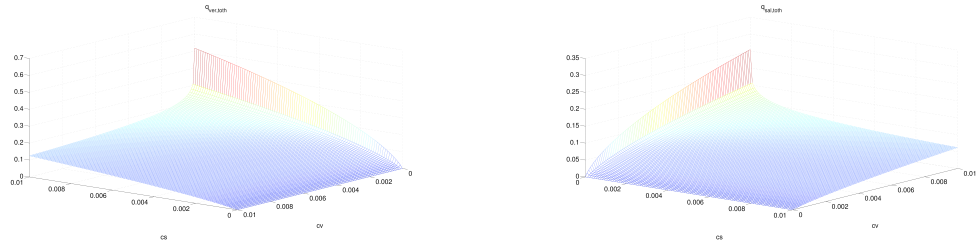

Figure 5.10: Toth binary isotherms

- Lower percentage of organic modifier in the mobile phase leads to a larger reduction in the effective column volume.

The first two items are highly correlated, and can be explained by the fact that the injected species are concentrated at the beginning of the column, which has the capacity of a finite number of moles. Since the number of injected moles are dependent on both injection volume and injection concentration, the same effect is observed if either one is increased. When the amount of organic modifier was reduced, a larger reduction in volume was observed, however, calculated in percentages, the effect is almost the same. The effect is expected to be more significant for lower amounts of organic modifier, since the relative advective transport is reduced, which would increase the relevance of competing adsorption. The bands of solutes are concentrated in the same volume, and are, thus, forced to compete for vacant sites.

5.3.3 Discussion - Competing adsorption

The investigation in this paper was performed with model compounds, and several differences can be expected when comparing to the preparative separation of real wood bio-polymers. Wood bio-polymers are expected to have a

very broad range of distribution, both regarding molecular weight (M_w) [17, 55] and aromatic content [18]. This characteristic would increase the risk of co-eluting species, and thus, increase competitive adsorption. However, the broad range of distribution would mean that the individual solute-bands that form during migration, are of rather low concentration, and thus reduce competing adsorption. The broad range of distribution in M_w would have an effect on the mass-transport resistance in chromatography. Diffusion resistance increases with M_w, which restricts the accessible volume of the stationary phase and adds to column dispersion. The solubility of wood bio-polymers is known to be reduced with increasing M_w.

The solubility of salicin restricted the experiments of this study. The aqueous solubility of salicin is 0.125 M at 15 ^0C and 0.874 M at 60 ^0C, while veratryl alcohol is fully miscible (Chemblink.com).

5.4 Paper IV

The purpose of the investigation in Paper IV was to estimate the productivity effect of varying sorbent particle size and solute molecular weight. The investigation also aimed to estimate the cost of separation and to suggest future work.

HETP was calculated for different flow velocities using Equation 4.3 and is presented in Figure 5.11, where HETP is plotted against the particle Peclet number, Pe_P. The particle diameter and the solute molecular weight were set constant to the values of the experimental conditions presented in Westerberg and Rasmuson [33] in the calculations, i.e. 70 μm and 1 kDa, respectively.

The value of HETP was at minimum at a Pe_P of around 60, which would be the value of optimal separation. A low Pe_P number is achieved by maintaining a low flow rate, small particle diameter or by separating low molecular weight species that have low diffusional resistance.

Figures 5 to 8 in Paper IV show that small molecules are easily separated on a relatively short column, while large polymers must be separated by using either small-diameter sorbent particles or very long columns. Increasing the flow rate significantly increases the required column length, as does increasing the purity requirement.

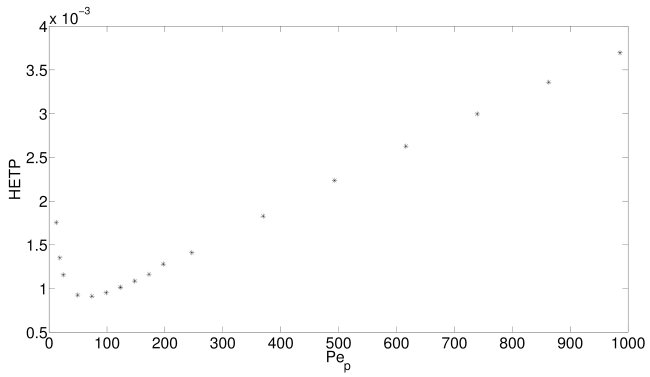

Figure 5.11: HETP as a function of particle Peclet number

Large-scale chromatographic separation is usually restricted by induced pressure drop over the column. The Ergun equation (Equation 2.30) was used to estimate the pressure drop at various flow rates, particle diameters and column lengths. The findings show that there was a significant difference in pressure drop between 5-20 μm in particle diameter. Using particles with diameters above 20 μm did not have a major influence on the pressure drop, Figure 5.12. An increased flow rate had a double effect on the pressure drop because it also increased column dispersion, and thereby the necessary column length. Despite this, the influence of the flow rate only became apparent at particle diameters exceeding 20 μm, since the particle diameter effect was markedly dominant at smaller particle sizes.

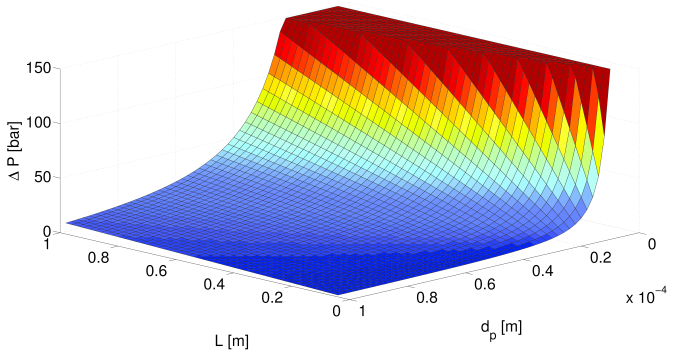

Figure 5.12: Pressure drop as a function of particle diameter and column length

The calculations show that the induced pressure drop is below the expected maximum, 15 MPa, except at very high MwD and d_p. At simultaneous extreme

values of MwD and d_p, the minimum column length exceeded the maximum simulated, and therefore the pressure drop could not be estimated.

The Biot number (Equation 2.25) was calculated for the simulations of extreme values, to ensure that the assumption of negligible film transport resistance was valid. The lowest value of the Biot number was about 20, and was found for the simulation of the lowest flow rate and lowest molecular weight species. This confirms that the particle internal diffusion resistance is the dominant resistance, which increases especially with increasing molecular weight.

5.4.1 Productivity

The estimates of production capacity and costs were based on relative terms and not on actual process conditions. The purpose of the estimates was to compare how the factors of sorbent particle radius and molecular weight of the target solutes affect process economy.

Production rate can be estimated with the data gathered from the simulations. Equation 5.6 was used to estimate the production of two fractions of 95 % pure biopolymers with the mobile-phase velocity of 0.0029 m/s, which corresponds to the laboratory setup conditions. Data from an experimentally verified case was used to produce a reference value of possible production.

$$Prod = \frac{C_{in}V_{in}}{A_c L t_e} \quad \left[\frac{mol}{m_C^3 h}\right] \tag{5.6}$$

where C_{in} and V_{in} are the concentration and volume of the solute pulse that is injected on the column. A_c is the cross sectional area of the column and L is the column length. t_e is the elution time of the second solute in the binary separation, given the specific conditions. m_C^3 refers to the column volume.

Productivity and production costs are estimated in three different cases. The experimental case used model compounds of molecular weights of about 1 kDa, sorbent particle diameters of a mean value of 70 μm, an injection volume of 50 μL and an injection concentration of 10^{-5} M, which was verified to be within the linear part of the isotherm [49]. The required column length and elution time were taken from the simulations and were 45 mm and 2400 s, respectively. The production capacity of this case (Case 1) would be 0.001 $mol/m_C^3, h$ of each component.

Case	d_p μm	M_W kDa	t_{elute} s	L_{min} m
1	70	1	2400	0.045
2	20	1	600	0.013
3	20	100	1600	0.031

Table 5.5: Parameter values used in calculation of process efficiency

To examine the production effect of sorbent-particle-size-induced dispersion, a second case (Case 2) was calculated with a mean particle diameter of $20\mu m$. The lower particle diameter reduces dispersion while still not inducing high pressure drop over the column (Figure 5.12). The simulations show that both column length and elution time were reduced to 12.5 mm and 600 s, respectively. The production capacity for this case increased to 0.0144 $mol/m_C^3, h$. The decrease in dispersion accounts for a production increase of a factor of 14. To estimate the effect of dispersion caused by higher molecular weight, a third calculation (Case 3) was made using the parameter values of Case 2 and increasing the molecular weight to 100 kDa. Simulations showed that the required length in Case 3 was 31 mm and the required elution time was 1600 s. The production rate in case 3 would be 0.0022 $mol/m_C^3, h$, which corresponds to a mass production rate of 220 $g/m_C^3, h$. Table 5.5 gives a summary of the settings for each of the cases.

Case	Production $\frac{mol}{m_C^3 h}$	Cost $\frac{m_l^3}{m_C^3 h}$
1	0.001	80
2	0.0144	289
3	0.0022	115

Table 5.6: Results of process production and cost estimates

Liquid consumption was calculated to estimate comparative separation costs in each of the cases. In all three cases, the flow velocity was the same, but since the column length varied, the column dimensions differed and thus also the flow rates. The consumption of liquid in Cases 1,2 and 3 was 80, 289 and 115 $m_l^3/m_C^3, h$. In terms of production costs, the values would be 40, 10 and 0.27 $m_l^3/g_{product}$. Table 5.6 presents a summary of production capacity and production costs for the various cases.

The injection concentration in Case 3 is likely to be above the linear part

of the isotherm, since the high molecular weight both reduces solubility due to an increase in entropy, and is expected to suffer steric blocking of adsorption sites in the sorbent particles.

For lower molecular weight solutes, the productivity and production costs can be improved by overloading the column, using gradient elution or changing flow velocity.

5.4.2 Discussion - Process economy

When moving from the ideal conditions of chromatographic separation of wood model constituents of Westerberg and Rasmuson [33] (Paper II) to include the practical implications of the complexity of native biopolymers, it is clear that the efficiency of separation is negatively affected. The value of biopolymers such as GGM or xylan is largely related to the number of repeating units of the polymer. It is likely that the same is true for LCCs and lignin polymers, but since the uses of these biopolymers has not been investigated to the same extent as polysaccharides, this is not certain. However, increasing molecular weight, which can be translated into an increased hydrodynamic radius of the polymers, has a significant effect on the effective diffusivity in the porous particles. The reduction in effective diffusivity might mean an inefficient use of column volume if the full volume of the particles does not reach equilibrium with the mobile phase. Moreover, the greater mass transfer resistance adds to the column axial dispersion, leading to longer columns or reduced resolution of the species.

The conditions at which separation is anticipated to take place, are similar to those of protein separation applied by the pharmaceutical industry. The difference between proteins with pharmaceutical utilisation and biopolymers from wood is, however, huge in respect to market value. While a protein can be worth thousands of Euro per gram, a wood biopolymer for the production of polymeric materials, similar to those of petroleum-based plastics, might be worth tens of Euros per kilogram. With these economic aspects in mind, it seems unreasonable to consider chromatographic means to separate wood biopolymers for material production. The economic conditions may, however, change over time. The process is not likely to ever compete for a position

in material production, but there may be components with higher value that cannot be extracted by other means.

While the technology seems inappropriate for use in material production, the technology has shown great potential for use within fundamental science. Instead of optimising separation for specific bio-polymers, it is suggested that a flexible method is developed, which can be adjusted to separate biopolymers of a variety of molecular weights and hydrophobicity. The purpose would be to characterise various constituents of wood and, by semi-preparative means, purify constituents to enable the identification and production of wood-active enzymes for a future biorefinery process.

The results show the necessity to combine different means of separation to obtain pure fractions of wood biopolymers. The molecular weight of the species has an effect on the efficiency of separation, which in some cases might be as important as the solutes´ difference in affinity for the sorbent. With this in mind there should be a preceding steric separation to obtain fractions of uniform size, as was used in Westerberg et al. [42] (Paper I).

6

Conclusions and Outlook

6.1 Conclusions

This research has shown that it is possible to separate hemicelluloses, lignin and LCCs by means of hydrophobic sorption. An experimental study applied cross-flow filtration followed by two sequential stages of hydrophobic sorption on a water suspension of wood polymers. This process separated the species according to their respective hydrophobicity.

The study in Paper I showed that it is necessary to combine separation methods. Membrane separation was employed prior to chromatographic separation in order to obtain monodisperse fractions.

In Paper II, a mathematical model was created, which describes the chromatographic separation of wood constituents well. The model can be used in method development and optimisation.

The study in Paper III showed that competing adsorption is not likely to be a limiting factor in preparative application. The main reason for this is that the solubility of the target biopolymers is low in comparison to the number of active sites in the stationary phase.

Simulations in Paper IV showed that it is crucial to use low diameter particle sorbents in order to avoid high-particle-Peclet-number-induced dispersion. Calculations showed that particle dimensions of 15-20 μm induced an acceptable level of dispersion, while not causing too high of a pressure drop through restricted flow.

The increased molecular weight of biopolymers reduces diffusivity, which causes dispersion in the same way as a large sorbent particle radius would. Consequently, the results of the study show that the production rate decreases with increasing molecular weight. The dispersion effect of large particle radius and high molecular weight species are, in extreme cases, as significant as the differences in affinity of the species for the stationary phase.

The economic estimations made in Paper IV indicate that there are currently no justifiable motives to separate wood biopolymers for material production by means of chromatography.

6.2 Outlook

This research has shown the possibility of separating wood biopolymers by the use of chromatography, and it investigated the influence of a number of physical phenomena which are likely to effect the separation. However; the effect of poly-dispersity, regarding both molecular weight and aromaticity, is still mainly uncharted territory.

The aqueous solubility of biopolymers consisting of polysaccharides containing aromatic groups has not been extensively investigated. The reason for this is, obviously, that these types of biopolymers have not been fractionated in preparative scale.

This research has shown that there are, today, no economic incentives to develop a large-scale chromatographic separation unit with the purpose of fractionating large amounts of biopolymers for the production of new materials. There are, however, large gaps of knowledge concerning the composition and chemical structure of the biopolymers that constitute wood. It is, therefore, suggested that future efforts aim to develop a flexible method of chromatographic separation for the purpose of fractionating and characterising biopolymers. The contents of this thesis can assist in this development, but the major research effort would be focused on laboratory work and development of prepurification methods.

Bibliography

[1] ASPO, www.aspousa.org, 2012.

[2] WWSC, www.wwsc.se, 2010.

[3] M. S. Lindblad, E. Ranucci, A. C. Albertsson, Macromolecular Rapid Communications 22 (2001) 962–967.

[4] M. Grondahl, L. Eriksson, P. Gatenholm, Biomacromolecules 5 (2004) 1528–1535.

[5] J. Hartman, A. C. Albertsson, J. Sjoberg, Biomacromolecules 7 (2006) 1983–1989.

[6] A. Bjorkman, Nature 174 (1954) 1057–1058.

[7] T. Koshijima, T. Watanabe, Association between lignin and carbohydrates in wood and other plant tissues, Springer Velag, Berlin, Heidelberg, New York,, 2003.

[8] J. Azuma, N. Takahashi, T. Koshijima, Carbohydrate Research 93 (1981) 91–104.

[9] M. Lawoko, G. Henriksson, G. Gellerstedt, Holzforschung 60 (2006) 156–161.

[10] Y. Uraki, Y. Usukura, T. Kishimoto, M. Ubukata, Holzforschung 60 (2006) 659–664.

[11] P. Oinonen, D. Areskogh, G. Henriksson, Carbohydrate polymers 95 (2013) 690–6.

[12] T. Persson, H. Krawczyk, A. K. Nordin, A. S. Jönsson, Bioresource Technology 101 (2010) 3884–3892.

[13] A. Andersson, T. Persson, G. Zacchi, H. Stalbrand, A. S. Jonsson, Applied Biochemistry and Biotechnology 137 (2007) 971–983.

[14] K. Leppänen, P. Spetz, A. Pranovich, K. Hartonen, V. Kitunen, H. Ilvesniemi, Wood Science and Technology 45 (2010) 223–236.

[15] S. H. Lin, R. S. Juang, Journal of Environmental Management 90 (2009) 1336–1349.

[16] M. Ek, Ljungberg textbook. Pulp and paper chemistry and technology. Book 2, Pulping chemistry and technology, Fiber and Polymer Technology, KTH, Stockholm, 2007.

[17] T. Song, A. Pranovich, I. Sumerskiy, B. Holmbom, Holzforschung 62 (2008) 659–666.

[18] N. Takahashi, J. I. Azuma, T. Koshijima, Carbohydrate Research 107 (1982) 161–168.

[19] H. H. Brownell, Tappi Journal 53 (1970) 1278–1281.

[20] S. Azhar, Y. Wang, M. Lawoko, G. Henriksson, M. Lindström, Bioresources 6 (2011) 4606–4614.

[21] K. Jedvert, Y. Wang, A. Saltberg, G. Henriksson, M. E. Lindström, H. Theliander, Nordic Pulp & Paper Research Journal 27 (2012) 828–835.

[22] D. Ruthven, Principles of Adsorption and Adsorption Processes, Wiley, New York, 1984.

[23] G. Guiochon, A. Felinger, D. Shirazi, A. Katti, Fundamentals of preparative and nonlinear chromatography, Elsevier, San Diego, CA, 2006.

[24] E. J. Wilson, C. J. Geankoplis, Industrial & Engineering Chemistry Fundamentals 5 (1966) 9–14.

[25] E. Cussler, Diffusion - mass transfer in fluid systems, Cambridge University Press, Cambridge, 3rd edition, 2009.

[26] C. Wilke, P. I. N. Chang, A.I.Ch.E. Journal (1955) 264–270.

[27] M. Suzuki, Adsorption Engineering, Elsevier, Amsterdam, 25 vol edition, 1990.

[28] S. Viel, D. Capitani, L. Mannina, A. Segre, Biomacromolecules 4 (2003) 1843–7.

[29] S. F. Chung, C. Y. Wen, AIChE Journal 14 (1968) 857–866.

[30] H. Darcy, Les Fontaines Publiques de la Ville de Dijon, Victor Dalamont, Paris, 1856.

[31] T. H. Chilton, A. P. Colburn, Trans. Am. Inst. Chem. Eng. 26 (1931).

[32] S. Ergun, Chemical engineering progress 48 (1952).

[33] N. Westerberg, A. Rasmuson, Chemical Engineering Research and Design 92 (2014) 1363–1370.

[34] G. M. Schwab, Ergebnisse der Exakten Naturwissenschaften, Julius Springer, Berlin, vol. 7 edition, 1928.

[35] E. Markham, E. Benton, J. Am. Chem. Soc. 53 (1931) 497–507.

[36] J.-X. Huang, G. Guiochon, Journal of Colloid and Interface Science 128 (1989) 577–591.

[37] S. Golshan-Shirazi, J.-x. Huang, G. Guiochon, Analytical Chemistry (1991) 1147–1154.

[38] a. Cavazzini, K. Kaczmarski, P. Szabelski, D. Zhou, X. Liu, G. G. Guiochon, Analytical chemistry 73 (2001) 5704–15.

[39] L. F. Shampine, M. W. Reichelt, Siam J. Sci. Comput. 18 (1997) 1–22.

[40] A. Wigell, H. Brelid, H. Thellander, Nordic Pulp & Paper Research Journal 22 (2007) 495–499.

[41] M. Lawoko, A. Nutt, H. Henriksson, G. Gellerstedt, G. Henriksson, Holzforschung 54 (2000) 497–500.

[42] N. Westerberg, H. Sunner, M. Helander, G. Henriksson, M. Lawoko, A. Rasmuson, Bioresources 7 (2012) 4501–4516.

[43] L. R. Snyder, J. J. Kirkland, J. W. Dolan, Introduction to modern liquid chromatography, Oxford: Wiley-Blackwell, 3rd edition, 2010.

[44] B. Y. H. Kubota, S. Tsuda, The Review of Physical Chemistry of Japan 49 (1979).

[45] J. M. Jacobson, J. H. Frenz, C. Horváth, Industrial and Engineering Chemistry Research 26 (1987) 43–50.

[46] J. Zhu, A. M. Katti, G. Guiochon, Journal of Chromatography A 552 (1991) 71–89.

[47] P. Valentin, G. Guiochon, Journal of Chromatographic Science 14 (1976) 56–63.

[48] N. Marchetti, A. Cavazzini, L. Pasti, F. Dondi, Journal of Separation Science 32 (2009) 727–741.

[49] N. Westerberg, A. Rasmuson, Chromatographic separation of wood model constituents : Analysis and modelling of competing adsorption, 2015.

[50] J. van Deemter, F. Zuiderweg, A. Klinkenberg, Chemical Engineering Science 5 (1956) 271–289.

[51] S. Willfor, R. Sjoholm, C. Laine, M. Roslund, J. Hemming, B. Holmbom, Carbohydrate Polymers 52 (2003) 175–187.

[52] M. Lawoko, Lignin polysaccharide networks in softwood and chemical pulps: charaterisation, structure and reactivity, Ph.D. thesis, Royal institute of technology, Stockholm, 2005.

[53] S. Willfor, P. Rehn, A. Sundberg, K. Sundberg, B. Holmbom, Tappi Journal 2 (2003) 27–32.

[54] W. R. Melander, Z. E. Rassi, C. Horváth, Journal of Chromatography A 469 (1989) 3–27.

[55] P. Oinonen, D. Areskogh, G. Henriksson, in: Proceedings of the 16th ISWFPC, Tianjin, pp. 1028–1031.